SISSA  **ISAS**

SCUOLA INTERNAZIONALE SUPERIORE DI STUDI AVANZATI

INTERNATIONAL SCHOOL FOR ADVANCED STUDIES

Matter-wave solitons for one-dimensional Bose gases

Thesis submitted for the degree of

"Doctor Philosophiæ"

Candidate:

Enrico Fersino

Supervisors:

Prof. Giuseppe Mussardo

Dr. Andrea Trombettoni

External referees:

Prof. Luca Salasnich

Prof. Pasquale Sodano

September 2008

Contents

Chapter 1

Introduction

Thirteen years after the first experimental observation of a Bose-Einstein condensed state (BEC) [1] in a dilute Bose gas of alkali atoms, the study of ultracold quantum systems has become a well established and active area of research in contemporary physics [2, 3] which encompasses a number of different fields like atomic, condensed matter and nuclear physics.

The continuous refinements of experimental techniques, recently reported both in bosonic and fermionic systems [4, 5], have allowed to achieve BEC states not only for the historical ^{87}Rb, ^{7}Li and ^{23}Na, but also for more complex systems like metastable ^{4}He, ^{85}Rb, ^{41}K, ^{123}Cs and spin-polarized hydrogen.

The experimental procedure needed to reach temperatures of order $10 - 100\, nK$ for dilute atomic gases can be summarized in essentially two distinct steps. The atoms are first collected in a magnetic-optical trap and cooled to micro-Kelvin temperature [6]. Then the nano-Kelvin temperature range is reached by evaporative cooling in a magnetic trap. This is the temperature range where the phenomenon of Bose-Einstein condensation (BEC) may occur: in fact the de Broglie wavelength of the bosons

$$\lambda_{dB} = \sqrt{\frac{2\pi\hbar^2}{m k_B T}} \tag{1.0.1}$$

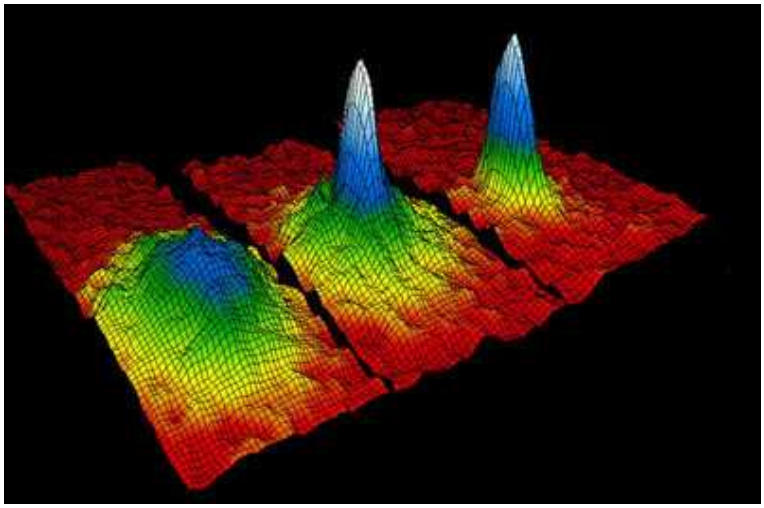

Figure 1.1: The velocity distribution of ultracold rubidium atoms after an expansion performed at JILA [1]. From left to right, the temperature of the system is decreased from $400nK$ to $50nK$, and a condensate - a macroscopic population of the ground state - appears. The left most frame has the negligible condensate fraction since it is just above the transition temperature. In the right most expansion, nearly all of the atoms are condensed, corresponding to the sharp peak. Taken from [7]

is comparable or larger than the average interparticle spacing, leading to a macroscopic occupation of a single quantum state, i.e. the BEC. This is a low temperature phase transition caused by pure statistical quantum effects.

After cooling, the velocity distribution of the atoms can be examined by performing a time-of-flight analysis. Fig. 1.1 shows the momentum distribution for systems with three different temperatures, one just above the transition temperature at 400nK and two below the transition temperature at 200nK and 50nK respectively, observed by the JILA group [1].

The two peculiar features of BEC systems are the extremely low temperature and density. The joint effect of these conditions results in weakly

microscopic interactions which, in turn, are the key to experimentally control the system parameters. In fact, in this regime the two-body interaction can be described by a single parameter, the s-wave scattering length a. Small values of a indicate a weak coupling between the particles, whereas its sign is responsible for the type of interactions, being repulsive for $a > 0$ and attractive when $a < 0$. In this respect, a substantial breakthrough has been made by the implementation of the so called Feshbach resonances technique [8]. Through this technique, which will be discussed in the second section of this chapter, it is indeed possible to control the sign of the scattering length, providing thus an effective tool to pass from the attractive regime to the repulsive one and vice versa.

Another very interesting aspect of ultracold atoms is the possibility to realize quasi-one dimensional gases. In particular, the jointly use of Feshbach resonances technique and optical lattices (OL) [9] made possible to investigate famous one-dimensional toy models like the one-dimensional Bose gas, i.e. Lieb-Liniger model [10, 11], and its hard core limit [12]. At variance with the case of higher dimensions, for such a systems several nonperturbative methods have been developed [13], so that in some cases direct comparisons between experiments and exact solutions can be made. Among these models, a special role is played by the integrable ones and their non-integrable extensions. In several instances, as we will see in Chapters 2-3, a comparison of different approaches in integrable models provides useful insights to treat the corresponding non-integrable version.

Quasi-one-dimensional Bose gases are obtained by using a cigar-shaped external trapping potential, elongated in one direction, with the other degrees of freedom frozen by a tight transverse confinement. Several variants of the interacting Bose gas in one dimension have been implemented in the experiments: an optical lattice was added to detect the Mott-superfluid transition in one dimension [14], the effective one-dimensional interaction

was tuned [15] to observe a Tonks-Girardeau gas of ultracold atoms [16, 17], or to study the effect of temperature [18].

Besides the possibility to modify the geometry and tune the interaction strength of the system, it has recently raised the challenging question of how it can be implemented an effective N-body interaction. Several proposals have recently addressed the issue of inducing and controlling three-body terms. In [19] it has been proposed to use cold polar molecules driven by microwave fields to obtain strong three-body interactions, controllable in a separate way from the two-body interactions, which in turn can be switched off [19]. Three-body interactions can be effectively induced in mixtures of bosonic particles and molecules: in [20] the ground state of rotating Bose gases close to a Feshbach resonance has been studied, showing that for suitable parameters they are fractional quantum Hall states, whose excitations obey non-abelian exchange statistics. In [21] it was shown that a system of atoms and molecules in a one-dimensional lattice can be effectively modeled by a three-body local (i.e., contact) interaction, characterized by a strength U and in the limit $U \to \infty$ (without a two-body interaction) the ground state properties were investigated by a Pfaffian-like ansatz. One of the main reasons of interest of these proposals relies on the fact that exotic quantum phases, such as topological phases, appear to be ground states of a Hamiltonian with three or more body interaction terms, an example being the fractional quantum Hall states described by the Pfaffian wavefunctions [22]. The excitations of Pfaffian states are non-abelian anyons, on which schemes of fault-tolerant topological quantum computations are based [23].

Despite the theoretical attractiveness this issue might generate, very few methods can be used to deal with this kind of systems. In fact, apart from some ingenious procedures which have been used for specific Hamiltonians [21] and perturbative methods, a very useful tool which can be used is the Hartree-Fock (HF) mean-field approximation.

In this approximation, the one dimensional Bose gas with two-body contact interactions is well described by the Gross-Pitaevskii (GP) equation, which has the form of a cubic nonlinear Schröedinger equation (NLSE). In one dimension the GPE is a completely integrable equation, which can be explicitly solved by means of the inverse scattering transform (IST) method [24, 25]. The GP equation admits soliton solutions in both repulsive and attractive cases: in the repulsive case the soliton solutions appear as local density depletions (grey or dark solitons), while for attractive interactions they appear like bright matter waves (bright solitons). However, the introduction of an external potential breaks, apart a few specific cases [26, 27, 28], the integrability of the system preventing the possibility to find any analytical solution. In the most interesting cases of harmonic traps and optical lattices a very useful tool to detect low energy properties of the systems turned out to be the variational approach [29].

In this thesis we will focus on the effect N-body contact interactions generate on a one-dimensional dilute system of weakly interacting Bose atoms, both in homogeneous case and in presence of external potentials. The plan of the thesis is the following:

- In the first chapter we introduce the mean-field theory for weakly interacting Bose gases and related Gross-Pitaevskii equation in the more general case. After a brief presentation of the variational approach, needed for the analysis of the low energy properties in presence of external potentials, we briefly discuss the technique of Feshbach resonances and how it is possible to realize quasi-one dimensional ultracold systems.

- The second chapter will be focused on integrable techniques for one dimensional Bose gases. After discussing its Bethe ansatz solution both for repulsive and attractive case, we present the classical inverse

scattering method (IST) to find the one-soliton solution of its mean-field theory, i.e. the 1D cubic nonlinear Schröedinger equation.

- In the third chapter, after introducing the mean-field theory of 1D attractive boson gases with N-body contact interactions, we study the ground state of the system and discuss its peculiarity in terms of N. After showing the singularity of three-body interactions, the effect of a harmonic trap is analyzed.

- In the last chapter we discuss the effect of an optical lattice (OL) on the ground state properties of 1D ultracold bosons with three-body attractive interactions, studying in particular the effects of the presence of a residual two-body interaction. After studying the soliton solutions of its mean-field counterpart, i.e. the 1D cubic-quintic Gross-Pitaevskii equation, a variational stability analysis is presented in presence of both an OL and harmonic trap.

- The paragraph on the perspectives closes the work.

1.1 Mean-Field Theory: the Gross-Pitaevskii Equation

Studying the stationary and dynamical properties of N interacting bosons is in general a very complicated problem. However, in the standard context of a weakly interacting Bose-Einstein condensate it is still possible to implement a satisfactory mean-field theory [2, 3, 6], enabling us to extract useful informations on the low energy properties.

Let us consider a bosonic system of N particles, of mass m, interacting through a two-body potential $U(\mathbf{r} - \mathbf{r}')$ and assume to be loaded in an external potential $V_{ext}(\mathbf{r})$. In the formalism of second quantization its

Hamiltonian is given by

$$\hat{H} = \frac{\hbar^2}{2m}\int d\mathbf{r}\nabla\hat{\Psi}^\dagger(\mathbf{r})\nabla\hat{\Psi}^\dagger(\mathbf{r}) + \int d\mathbf{r}\hat{\Psi}^\dagger(\mathbf{r})V_{ext}(\mathbf{r})\hat{\Psi}(\mathbf{r}) + \frac{1}{2}\int d\mathbf{r}\, d\mathbf{r}'\hat{\Psi}^\dagger(\mathbf{r}')\hat{\Psi}^\dagger(\mathbf{r}')U(\mathbf{r}-\mathbf{r}')\hat{\Psi}(\mathbf{r})\hat{\Psi}(\mathbf{r}') \quad (1.1.1)$$

where $\hat{\Psi}^\dagger(\mathbf{r}), \hat{\Psi}^\dagger(\mathbf{r})$ are field operators satisfying the canonical equal-time commutation relations:

$$\left[\hat{\Psi}^\dagger(\mathbf{r}), \hat{\Psi}(\mathbf{r}')\right] = \delta(\mathbf{r}-\mathbf{r}'), \quad \left[\hat{\Psi}(\mathbf{r}), \hat{\Psi}(\mathbf{r}')\right] = 0, \quad \left[\hat{\Psi}^\dagger(\mathbf{r}), \hat{\Psi}^\dagger(\mathbf{r}')\right] = 0$$

In this representation, the equation of motion for the time-dependent field operator is given by

$$i\hbar\frac{\partial\hat{\Psi}(t)}{\partial t} = \left[\hat{\Psi}(t), \hat{H}\right] \quad (1.1.2)$$

Now, by resorting to the hypothesis of the Born approximation we can replace the two-body interatomic potential with an effective local potential $U(\mathbf{r}-\mathbf{r}') \approx U_0 \cdot \delta(\mathbf{r}-\mathbf{r}')$, where $U_0 = 4\pi\hbar^2 a/m$ and a is the s-wave scattering length. At very low temperature, in the regime of weakly interparticle interactions we can safely assume the system to be in a state close to a BEC state, in such a way the field operator may be written as

$$\hat{\Psi}(\mathbf{r}, t) = \Psi(\mathbf{r}, t) + \hat{\Psi}'(\mathbf{r}, t) \quad (1.1.3)$$

Here the scalar function $\Psi(\mathbf{r}, t)$, defined as the expectation value of the field operator in the grand canonical ensemble, represents the condensate wave function of the system, while with $\Psi'(\mathbf{r}, t)$ has been denoted the quantum corrections field.

Substituting (1.1.3) in (1.1.2), and neglecting the first order term, we finally get the time-dependent Gross-Pitaevskii equation (GPE) in the order parameter $\Psi(\mathbf{r}, t)$

$$i\hbar\frac{\partial}{\partial t}\Psi(\mathbf{r}, t) = -\frac{\hbar^2}{2m}\nabla^2\Psi(\mathbf{r}, t) + \left[V_{ext}(\mathbf{r}, t) + U_0 \mid \Psi(\mathbf{r}, t) \mid^2\right]\Psi(,t) \quad (1.1.4)$$

This mean-field equation has thus the form of a cubic nonlinear Schröedinger equation in an external potential. It is worth to notice that in presence of an external potential with a harmonic cylindrical symmetry, the 3D Gross-Pitaevskii equation reduces to an effective 1D nonlinear nonpolynomial Schröedinger equation [30]. Further, we remark that the nonlinear term $U_0 \mid \Psi(\mathbf{r},t) \mid^2$ and, as we will see in Chap. 3, the corresponding ground state properties strongly depend on the "microscopic process" involved. In this respect we want to point out that a tuning of the scattering length a, from positive to negative value, amounts to pass from a focusing to a defocusing regime, while the nonlinearity degree is related to the number of simultaneous microscopic interactions [31].

1.1.1 Variational approach

Apart from few cases [26, 27], solving explicitly the Gross-Pitaevskii equation, in presence of an external potential, turns out to be an impossible task. However some useful insights, on the low energy properties of trapped gases, are still achievable through a variational approach.

By assuming the system to be in a condensed state, i.e. the N-particle wave-function to be factorized $\Psi(\mathbf{r}_1,\mathbf{r}_2,...,\mathbf{r}_N) = \prod_{i=1}^{N}\psi(\mathbf{r}_i)$, the corresponding energy reads

$$E[\psi] = \int d\mathbf{r}\left[\frac{\hbar^2}{2m} \mid \nabla\psi(\mathbf{r}) \mid^2 + V_{ext}(\mathbf{r}) \mid \psi(\mathbf{r}) \mid^2 + \frac{1}{2}U_0 \mid \psi(\mathbf{r}) \mid^4\right] \quad (1.1.1)$$

In the BEC context, the variational approach results in minimizing the energy functional (1.1.1) with respect to independent variations of the single-particle wave function $\psi(\mathbf{r})$ and imposing the normalization condition on the total number of particles

$$N = \int_{-\infty}^{+\infty} \mid \psi \mid^2 d\mathbf{r}. \quad (1.1.2)$$

Taking care of this constraint by the method of Lagrange multipliers, the result is equivalent to minimize $E - \mu N$, where μ denotes the chemical potential of the system. Equating to zero the variation of this quantity we finally get

$$-\frac{\hbar^2}{2m}\nabla^2\psi(\mathbf{r}) + V_{ext}(\mathbf{r})\psi(\mathbf{r}) + U_0 \mid \psi(\mathbf{r}) \mid^2 \psi(\mathbf{r}) \;=\; \mu\psi(\mathbf{r}) \tag{1.1.3}$$

which is the time-independent Gross-Pitaevskii equation in the order parameter $\psi(\mathbf{r})$.

In order to appreciate the efficiency of the method, we shall illustrate how its application to a dilute trapped gas enable us to grasp its low energy properties. Let us suppose to consider a bosonic gas trapped in an anisotropic three-dimensional harmonic-oscillator potential

$$V_{ext}(x_1, x_2, x_3) \;=\; \frac{1}{2}\, m\, (\omega_1^2 x_1^2 + \omega_2^2 x_2^2 + \omega_3^2 x_3^2) \tag{1.1.4}$$

where $\omega_i, i = 1, 2, 3$ are real parameters, related to the characteristic oscillator lengths by $d_i = \sqrt{\hbar/m\omega_i}$.

By switching on microscopic interactions between the particles, we expect that the Gaussian wave function, exhibited by the system when no scattering process occurs, can modify its dimensions. Let us assume as variational ansatz the usual Gaussian wavefunction

$$\psi(x_1, x_2, x_3) \;=\; \frac{N^{1/2}}{\pi^{3/4}(\sigma_1\sigma_2\sigma_3)^{1/2}}\, e^{-x_1^2/2\sigma_1^2 - x_2^2/2\sigma_2^2 - x_3^2/2\sigma_3^2} \tag{1.1.5}$$

where $\sigma_1, \sigma_2, \sigma_3$ play the role of variational parameters. The substitution of (1.1.5) into (1.1.1) yields the energy expression

$$E(\sigma_1, \sigma_2, \sigma_3) \;=\; N \sum_{i=1}^{3} \hbar\omega_i \left(\frac{d_i^2}{4\sigma_i^2} + \frac{\sigma_i^2}{4d_i^2} \right) + \frac{N^2 U_0}{2(2\pi)^{3/2}\sigma_1\sigma_2\sigma_3}, \tag{1.1.6}$$

which reaches its minimum at

$$\sigma_i \;=\; \left(\frac{2}{\pi^2}\right)^{1/10} \left(\frac{Na}{d_0}\right)^{1/5} \frac{\bar{\omega}}{\omega_i} d_0. \tag{1.1.7}$$

where $d_0 = \sqrt{\hbar/m\bar{\omega}}$ and $\bar{\omega} = (\omega_1\omega_2\omega_3)^{1/3}$. The ground state energy per particle thus becomes

$$\frac{E}{N} = K\left(\frac{Na}{d_0}\right)^{2/5}\hbar\bar{\omega} \tag{1.1.8}$$

where K is a numerical value given by $(5/4)(2/\pi)^{1/5}$. This variational estimate predicts that the energy per particle is proportional to $N^{2/5}$ when the kinetic energy is neglected, and of order $(Na/d_0)^{2/5}$ times greater than the energy in the absence of interactions in perfect agreement with the Thomas-Fermi approximation.

For the isotropic harmonic potential ($\omega_i = \omega$) , the energy reduces to the simpler expression [32]

$$E(\lambda) = \frac{N\hbar\omega}{2}\left[\frac{3}{2}(\lambda^2 + \lambda^{-2}) + \alpha\lambda^3\right] \tag{1.1.9}$$

where $\alpha \equiv \sqrt{2/\pi}(Na/d_0)$, $\lambda = d_0/\sigma$ is the dimensionless spatial size of the condensate and $\sigma \equiv \sigma_i$ is the remaining variational parameter. As shown in Fig.1.2, in the case of attractive interactions ($a < 0$) a local minimum exists provided N is less than some critical value N_c while for larger values of N a collapse is achieved. The critical particle number is given by

$$\frac{N_c \mid a \mid}{d_0} = \frac{2(2\pi)^{1/2}}{5^{5/4}} \approx 0.67 \tag{1.1.10}$$

which is in good agreement with the value 0.57 obtained by numerical integration of Gross-Pitaevskii equation [33].

1.2 Feshbach resonances

The idea which is behind the Feshbach resonance mechanism is to exploit the hyperfine structure, that certain species of atoms show, in order to change the colliding properties of gaseous systems. This phenomenon, which has been investigated a long time ago in the context of nuclear matter [8],

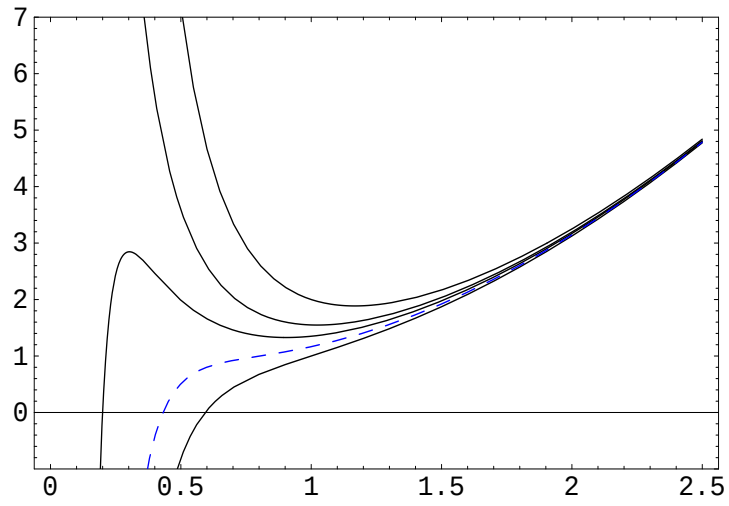

Figure 1.2: Variational expression for the energy per particle for an isotropic harmonic trap as a function of the variational parameter σ, for different values of the dimensionless parameter Na/d_0. The dashed line corresponds to the critical value, approximately -0.67, at which the cloud becomes unstable

has become essential for fermionic ultracold atoms to study the BCS-BEC crossover.

The two-body scattering process, between hyperfine species in a magnetic field B, can take place with different atomic states, the so called "channels" (set of quantum numbers) of interaction. As a rule, distinct channels have different magnetic moments μ and, accordingly, different zero-point energies (scattering threshold) so that $\Delta E = \Delta\mu \times B \neq 0$. Following the convention to call "open" and "closed" channels, those ones with the higher E_{op} and lower E_{cl} threshold respectively, the Feshbach mechanism occurs when a binding energy E_0 of the open channel is nearly resonant with the scattering threshold of the closed channel (vd.Fig. 1.3).

In the limit where detuning parameter $\delta \equiv E_0 - E_{cl}$ tends to zero, as a result of coupling between the channels, the scattering particles in the

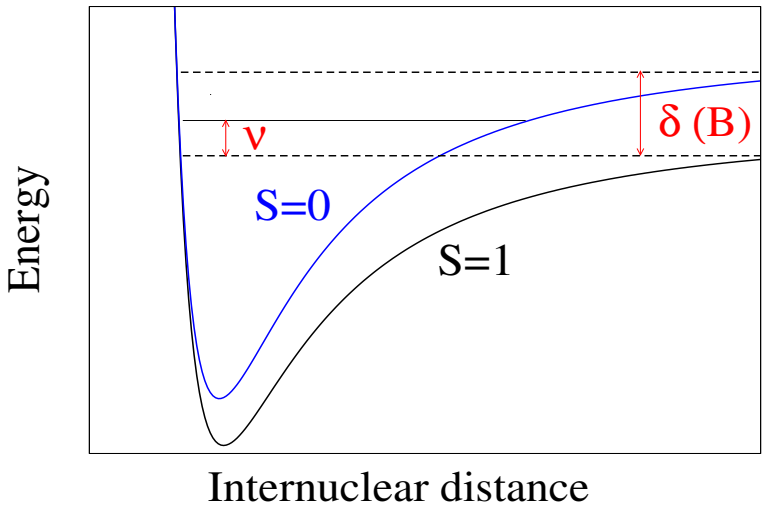

Figure 1.3: Pictorial description of a Feshbach resonance. The lower line corresponds to the potential between the two scattering atoms in the open channel and the upper to the interaction potential in the closed channel. The shift between the continuum states (represented with dashed lines) between open and closed channels due to magnetic field, corresponds to $\delta(B)$. The detuning parameter ν measures the difference between the bound state in the closed channel and the zero energy of the open one. Taken from [34].

closed channel are affected by the bound states in the open one. For such a reason, a suitable adjusting of the magnetic field makes it possible to vary δ from positive to negative values, resulting in a change of the effective scattering length with respect to its background, ruled by the equation

$$a = a_0 \left(1 - \frac{\Delta}{B - B_0}\right), \tag{1.2.1}$$

where Δ is the width of the resonance, a_0 the background scattering length and $B - B_0$ is proportional to the detuning parameter. In particular, an attractive ($a < 0$) interaction occurs when the kinetic energy of colliding particles is below the binding energy of the open channel, while a repulsive ($a < 0$) interaction is achieved in the opposite situation (vd. fig. 1.4).

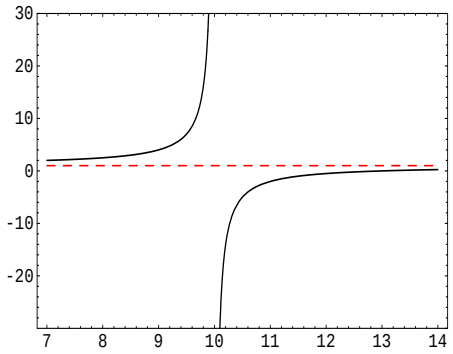

Figure 1.4: In this picture is shown the scattering length as a function of the magnetic field: positive (negative) values correspond to repulsive (attractive) interactions

We remark that the possibility to change the sign of the scattering length from positive to negative values have already allowed to observe and study the formation of bright solitons in Bose-Einstein condensates of ^{7}Li and ^{85}Rb as reported in [35, 36, 37, 38, 39, 40, 41, 42, 43]. On the other hand, several theoretical investigations on attractive condensates have shown richer stability properties with respect to the repulsive case [44, 45, 46]. As reported in the previous section, a critical threshold for the existence of bright solitons has been confirmed also in the case of non-local attraction, where a richer ranges of stability have been shown [47].

Together with the sign of interatomic interactions, in ultracold systems a crucial role is played both by the dimension of the system and the trapping potential.

In three dimensions, for instance, homogeneous attractive bosons with two-body interactions are unstable against the collapse, which can be prevented by means of an external harmonic trap provided that a critical particle number is reached. At variance, as we will see in chapter 3, in one dimension the addition of an harmonic trap always stabilizes the system irrespectively of the number of particles involved.

In the next section we will sketch in which way one-dimensional systems can be successfully realized in the experimental setups.

1.3 One-Dimensional Setups

The usual way to obtain quasi one-dimensional Bose gases is by trapping a three dimensional system in an external cigar-shaped trapping potential.

For the sake of simplicity, let us suppose to consider a two dimensional system loaded in a confining potential $U(x, y)$ with a privileged direction, say x, in such a way it can be approximated as $U_1(x) \cdot U_2(y)$, $U_2(y)$ being a freezing potential.

In these conditions the wave functions may thus be written as:

$$\psi(x, y) = e^{ikx}\varphi(y) \tag{1.3.1}$$

where φ is a localized state, whose shape depends on the form of the potential. In a simplified picture, if approximate the transverse potential as an infinite well of width l, as shown in 1.5, $\varphi(y) = \sin((2n_y + 1)\pi y/l)$ and the energy of the system reduces to

$$E = \frac{k_x^2}{2m} + \frac{k_y^2}{2m} \tag{1.3.2}$$

where k_x and k_y are the components of the momentum along homonymous directions. The finite size of the well results in a quantization of transverse energy (E_y), which in turn leads to energy minibands whose separation is at least

$$\Delta E = \frac{3\pi^2}{2ml^2} \tag{1.3.3}$$

see in Fig.1.5. Due to the narrowness of the transverse direction (typically of order of $60nm$ [48, 49, 50]), the values of k_y are sizable. Hence a one dimensional system is reached when the distance between the minibands

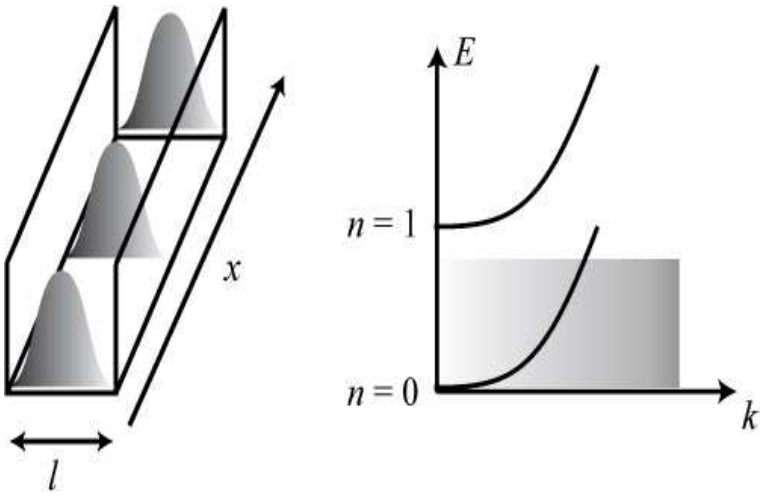

Figure 1.5: On the *left* is shown the density profile of a bosonic gas in a one-dimensional tube of transverse size l, propagating along the x direction. On the *right* it is drawn the dispersion relation $E(k)$, where k is the momentum along x, and the minibands resulting from the confining potential in the y direction. When the temperature, represented by the gray box, is below the miniband threshold only one miniband can be excited and the system behaves like one dimensional object. Taken from [9]

is adjusted to be larger than thermal temperature involved. When these conditions are achieved, the bosons are described by

$$H = \int dx \frac{\hbar^2 (\nabla\psi)^\dagger (\nabla\psi)}{2m} + \frac{1}{2}\int dx\, dx'\, U(x-x')\rho(x)\rho(x') - \mu_0 \int dx\, \rho(x) \tag{1.3.4}$$

where the first term is the kinetic energy, the second term is the interaction potential U between the bosons and the last term is the chemical potential μ_0. At low density, the interaction potential $U(x-x')$ can be approximated by a local interaction

$$V(x) = V_0\, \delta(x) \tag{1.3.5}$$

where V_0 is the effective interaction strength, resulting from the real three dimensional two-body interaction and the coupling with transverse degrees

of freedom. This model is the well-known Lieb-Liniger model which we will treat in the next section.

Together with the realization of confining traps, another very interesting experimental achievement has been the implementation of one dimensional optical lattices, which allowed to detect and study the one-dimensional quantum-superfluid–Mott-insulator phase transition [14]

The experimental setup usually consists of Bose gas (1.3.4) loaded in a periodic potential $V_L(x)$ coupled to the density [48]

$$H_L = \int dx\, V_L(x)\rho(x) \tag{1.3.6}$$

where

$$V_L(x) = \frac{V_L(1-\cos(2kx))}{2} \tag{1.3.7}$$

while V_L and $a = \pi/k$ are the depth and the width of the optical lattice.

In the high depth regime, i.e. when V_L is much higher than the kinetic energy, each minima of the lattice can be approximated by a harmonic well $2V_L k^2 x^2$. Hence, on each site, harmonic oscillator wavefunctions hybridize to form a band. If V_L is large enough, the energy levels in each trap are well separated so that one can retain only the ground state wavefunctions. The system can then be represented directly by the Bose-Hubbard model [13]

$$H = -J\sum_i (b_{i+1}^\dagger b_i + \text{h.c.}) + U\sum_i n_i(n_i-1) - \sum_i \mu_i n_i \tag{1.3.8}$$

where b_i ($b_i^\dagger$) destroys (creates) a boson on site i. The parameters J, U, and μ_i are respectively the effective hopping, interaction and local chemical potential. Because the overlap between different sites is very small the interaction is really local. Since atoms are neutral this model is a very good approximation of the experimental situation.

The effective parameters J and U can be computed by a standard tight binding calculation using the shape of the on site Gaussian wave function

$$\psi_0(x) = \left(\frac{m\omega_0}{\hbar\pi}\right)^{1/4} e^{-\frac{m\omega_0}{2\hbar}x^2} \tag{1.3.9}$$

where $\omega_0^2 = 4V_L k^2$. The result [9] is

$$\begin{aligned} J &= \langle \psi_0(x+a)|H_{\rm kin}|\psi_0(x)\rangle \\ U &= \int dxdydz|\psi(x,y,z)|^4 \end{aligned} \tag{1.3.10}$$

where $\psi(x,y,z) = \psi_0(x)\psi_\perp(y)\psi_\perp(z)$, $\psi_\perp$ is (1.3.9) and V_L has been replaced by the transverse confinement $V_\perp$. For large lattice sizes an approximate formula is given by [51]

$$\begin{aligned} J/E_r &= (4/\sqrt{\pi})(V_L/E_r)^{(3/4)} \exp\left(-2\sqrt{V_L/E_r}\right) \\ U/E_r &= 4\sqrt{2\pi}(a_s/2a)(V_L V_\perp^2/E_r^3)^{(1/4)} \end{aligned} \tag{1.3.11}$$

Here $E_r = \hbar^2 k^2/(2m)$ is the so called recoil energy, i.e. the kinetic energy for a momentum of order π/a, $V_\perp$ denotes the harmonic confining potential in the two transverse directions of the tube, while typical values for the remaining parameters are $a_s \sim 5nm$ and $a \sim 400nm$ respectively [48]. The repulsion term acts if there are two or more bosons per site. From eqn. (1.3.11) it is evident that the addition of an optical lattice is a simple way to freeze the kinetic energy of the system and leaving interactions practically unaffected.

Chapter 2

Integrable Methods for One-Dimensional Bose Gases

In this chapter we will introduce the Lieb-Liniger model for a one-dimensional Bose gas with two-body contact interactions and discuss the standard methods to solve it. This toy model, throughly studied starting from sixties [10], is an integrable model whose complete solution is given by means of the Bethe ansatz technique.

In the first section we will briefly remind essentials of coordinate Bethe Ansatz, as it has been developed in the seminal paper by Lieb and Liniger [10], and recover the ground state energy for both repulsive and attractive interactions. After pointing out the main differences of the two cases, we will concentrate on the attractive interaction, showing the limit which we have to keep in order to validate the Gross-Pitaevskii approximation. In the second section we will discuss the inverse scattering transform method (IST) in order to find the well known bright soliton solution for the nonlinear Schröedinger equation (NLE) in the focusing case (attractive interaction). This analysis will be carried out starting from a Zakharov-Shabat spectral problem.

2.1 Bethe Ansatz

The Lieb-Liniger model is a quantum one-dimensional (1D) system of N nonrelativistic bosonic particles interacting through a pairwise potential $\delta(x_i - x_j)$. In proper units the Hamiltonian is given by [10]:

$$H = -\frac{\hbar^2}{2m}\sum_{j=1}^{N}\frac{\partial^2}{\partial x_j^2} + 2c\sum_{\langle i,j\rangle}\delta(x_i - x_j) \tag{2.1.1}$$

where $\langle i,j\rangle$ represents the sum over all pairs, m is the mass of the particles and c the strength of the interaction, which mimics a repulsive interaction or an attractive one as $c > 0$ and $c < 0$ respectively. In terms of experimental parameters the 1D coupling constant is $c = -\hbar^2/ma_{1D}$, where a_{1D} is the effective 1D scattering length. For definiteness, let us suppose the system to be confined within a ring of length L (i.e. $0 \leq x_i < L$) in such a way periodic boundary conditions are reproduced. From sake of simplicity, let us fix natural units $\hbar = 2m = 1$ throughout.

In second quantization, this is nothing but the nonlinear Schrödinger theory for a canonical Bose field,

$$H = \int_0^L dx\left\{\partial_x\Psi^\dagger(x)\partial_x\Psi(x) + c\Psi^\dagger(x)\Psi^\dagger(x)\Psi(x)\Psi(x)\right\}. \tag{2.1.2}$$

which is a well-known integrable theory. The integrability of the model guarantees Yang-Baxter equations hold, these being signatures that the model does not have any "true" three-particle interaction. The physical content of this statement is that any scattering among three particles can be decomposed in consecutive scattering in pairs and, more crucially, the order in which these interactions take place is not important [52].

2.1.1 Repulsive interactions

Let us start by considering the case of N bosonic particles with a repulsive contact interaction. In this case no bound states are allowed since an infinite

energy should be necessary to overcome the δ-potential.

The Bethe Ansatz is based on the assumption that the eigenfunctions of the Hamiltonian can be expressed as a linear combination of plane waves, depending on a set of pseudo-momenta (or rapidities) $\{\lambda_1, .., \lambda_N\}$, that is

$$\Psi(x_1, .., x_N; \lambda_1, .., \lambda_N) \equiv \sum_P A_P \prod_{i=1}^{N} e^{i\lambda_{Pi} x_i}, \tag{2.1.1}$$

where it is understood that the sum runs over all permutations P of the parameters and A_P denotes a constant coefficient, depending on the permutation involved.

Because of bosonic nature of the system, a symmetry condition under exchange of coordinate guarantees that

$$\Psi(x_1, .., x_N; \lambda_1, .., \lambda_N) \equiv \Psi(x_{Q1}, .., x_{QN}; \lambda_1, .., \lambda_N) \tag{2.1.2}$$

for every permutation Q of the particles, reducing the problem to the sector $0 \leq x_1 \leq x_2 \leq ... \leq x_N < L$.

Due to the discontinuity of the wave function at $x_i = x_j$ we have that

$$H\,\Psi(\mathbf{x}, \lambda) = \left(\sum_{i=1}^{N} \lambda_i^2\right) \Psi(\mathbf{x}, \lambda) \tag{2.1.3}$$

$$+ 2 \sum_P \sum_{i,j=1}^{N} \delta(x_i - x_j)[i(A_{(Pi,Pj)} - A_{(Pj,Pi)})(\lambda_{Pi} - \lambda_{Pj}) - c(A_{(Pi,Pj)} + A_{(Pj,Pi)})]e^{i(\lambda_{Pi} - \lambda_{Pj})}$$

where with $(A_{(Pi,Pj)}$ and $(A_{(Pj,Pi)}$ we have denoted coefficients differing just by a transposition. Therefore the eigenvalue equation is satisfied provided that

$$\frac{A_{(Pi,Pj)}}{A_{(Pj,Pi)}} = -e^{-i\,\theta(\lambda_{Pi} - \lambda_{Pj})} \tag{2.1.4}$$

where

$$\theta(\lambda) \equiv -2 \arctan\left(\frac{\lambda}{c}\right) \tag{2.1.5}$$

represents the phase shift that the particles i and j have mutually exchanged during the interaction, while λ_{Pi} and λ_{Pj} are the corresponding rapidities.

The resulting energy is thus given by

$$E = \sum_{j=1}^{N} \lambda_j^2 \tag{2.1.6}$$

whereas the total momentum reads

$$P = \sum_{j=1}^{N} \lambda_j \tag{2.1.7}$$

Finally, by imposing periodic boundary conditions to the wave function

$$\Psi(x_1, x_2, .., x_j + L, .., x_N) = \Psi(x_1, x_2, .., x_j, .., x_N), \quad j = 1, .., N \tag{2.1.8}$$

we get the celebrated Bethe Ansatz equations for the rapidities

$$e^{i\lambda_j L} = \prod_{i \neq j} \left(\frac{\lambda_j - \lambda_i + ic}{\lambda_j - \lambda_i - ic} \right), \quad j = 1, ..., N. \tag{2.1.9}$$

By taking the logarithm, we end up to the equivalent set

$$\lambda_j L + \sum_k \theta(\lambda_j - \lambda_k) = 2\pi I_j, \quad j = 1, ..., N. \tag{2.1.10}$$

where the quantum numbers I_j are half-odd integers if N is even, and integers if N is odd. For the repulsive interaction ($c > 0$) it can be proved that, given a proper set of quantum numbers $\{I\}$, the solution of the Bethe equations for the set of rapidities $\{\lambda\}$ exists and is unique [53], due to the convexity of the Yang-Yang action associated with (2.1.10). Furthermore it can be proved that all solutions $\{\lambda\}$ are real [53]. The eigenfunctions of the Hamiltonian are thus given by the explicit expression [54]

$$\Psi_N(x_1, ..., x_N | \lambda_1, ..., \lambda_N) = \prod_{N \geq j > k \geq 1} sgn(x_j - x_k) \times$$
$$\sum_P (-1)^{[P]} e^{i \sum_{j=1}^{N} \lambda_{P_j} x_j + \frac{i}{2} \sum_{N \geq j > k \geq 1} sgn(x_j - x_k) \theta(\lambda_{P_j} - \lambda_{P_k})}, \tag{2.1.11}$$

where we have indicated by $[P]$ the signature of P. It is worth to note that these eigenfunctions identically vanish when two pseudo-momenta coincide,

reproducing a Pauli-like exclusion principle. Therefore all physical states are generated by a set of different quantum numbers I_j, conferring thus a fermionic nature to the system.

On the other hand, in the hard-core bosons, i.e. $c \to \infty$, corresponding to the Tonks-Girardeau limit (TG) [12], the pseudo-momenta space reduces to a lattice described by $\lambda_j = 2\pi I_j/L$. By assuming an even number of particles, the ground state is simply given by a set of integers symmetrically distributed around 0, so that the energy per particle reduces to

$$\frac{E_{TG}}{N} = \frac{2\pi^2}{3}\frac{N^2+3N+1}{L^2} \tag{2.1.12}$$

which is finite in the thermodynamic limit, i.e. when the number of particles N and the length of the box L tend to infinity so that their ratio $\rho = N/L$ remains finite.

2.1.2 Attractive interactions

Differently from the repulsive case, in presence of attractive interactions bound states are allowed, resulting in additional complex solutions to the Bethe equations. By putting $\bar{c} = -c > 0$ and assuming a complex value for rapidities we get

$$e^{i\lambda_\alpha L} = e^{i\lambda L - \eta L} = \prod_{\alpha\neq\beta}\frac{\lambda_\alpha - \lambda_\beta - i\bar{c}}{\lambda_\alpha - \lambda_\beta + i\bar{c}}. \tag{2.1.1}$$

If we keep N finite and let $L \to \infty$ we have that if $\eta > 0$, then $e^{-\eta L} \to 0$ on the left-hand side. So by looking at the finite product on the right-hand side, we conclude that there must be a rapidity $\lambda_{\alpha'}$ such that $\lambda_{\alpha'} = \lambda_\alpha - i\bar{c} + \mathrm{O}(e^{-\eta L})$, the same result we would obtain if $\eta < 0$. A general eigenstate is thus made by partitioning the total number of particles N into a set of N_s bound-states, each of which is characterized by its length j

$$N = \sum_j jN_j, \qquad N_s = \sum_j N_j, \tag{2.1.2}$$

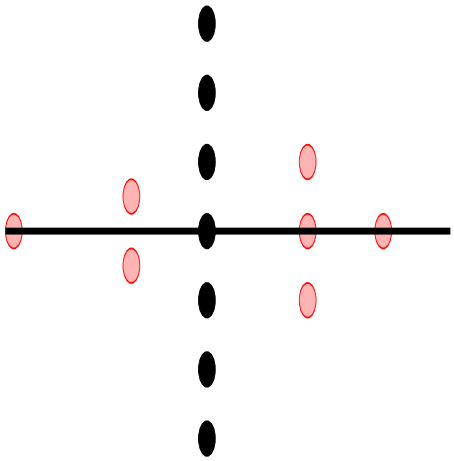

Figure 2.1: Two string states of a gas of $N = 7$ atoms. Black: The ground state consists of a single string centered at $k = 0$ with all the N particle aligned on the imaginary axis. Red: An excited states with 4 strings of length $j = 1, 2, 3$ and $N_1 = 2, N_2 = 1, N_3 = 1, N_{j>3} = 0$.

the rapidities being parametrized as

$$\lambda_\alpha^{j,a} = \lambda_\alpha^j + i\frac{\bar{c}}{2}(j + 1 - 2a) + i\delta_\alpha^{j,a} \qquad (2.1.3)$$
$$\delta \sim e^{-\gamma L}$$

where the index $a = 1, ..., j$ labels rapidities within the string, $\alpha = 1, ..., N_j$ labels string of a given length and γ is some positive constant (see Fig.**??**).

In this case, once we have fixed N, the limit $L \to \infty$ let the string states go to perfect arrangements still keeping them in strongly correlated states. The states are thus represented as fictitious particles with energy and momentum given by

$$E_{(j,\alpha)} = j(\lambda_\alpha^j)^2 - \frac{\bar{c}^2}{12}j(j^2 - 1), \qquad P_{(j,\alpha)} = j\lambda_\alpha^j \qquad (2.1.4)$$

behaving like soliton objects. The lowest energy state is reached by putting all particles in just one string centered on zero, that is

$$\lambda^{N,a} = i\frac{\bar{c}}{2}(N + 1 - 2a) + \mathrm{O}(\delta)\,. \qquad (2.1.5)$$

thus giving

$$E_{GS} = \sum_a (\lambda^{N,a})^2 = -\frac{\bar{c}^2}{12} N(N^2-1). \tag{2.1.6}$$

and a total momentum equal to zero. It is important to note that, unlike the repulsive case where the energy is not extensive, in presence of attractive interactions the ground state grows like N^3, thus reflecting the instability of the system in the thermodynamic limit.

In order to cure this pathology and keep the ground state finite it is now necessary to consider the unconventional limit of a large number of particles $N \gg 1$ with weak interactions $\bar{c} \ll 1$, such that $g = \bar{c}N$ remains finite and the energy per particle simply reduces to $E_{GS} = -g^2/12$.

2.2 Inverse scattering transform

In this section we briefly discuss the technique of the inverse scattering transform (IST) to find the so called *bright* soliton solution of the focusing nonlinear Schröedinger equation.

This method is essentially based on the complete integrability of the system, that is the existence of a linearized structure over the nonlinear evolution equation (NLEE) one is interested in. At the sight of the application, we will present the main steps of the procedure for NLEE involving potentials, let's say $\mathbf{q}$, depending on just one spatial dimension other then the temporal one. More formally, given a NLEE

$$\mathbf{q}_t \;=\; F(t, \mathbf{q}(x,t), \mathbf{q}_x, \mathbf{q}_{xx}, ...) \tag{2.2.1}$$

we define as Lax pair a couple of linear operators,

$$\begin{aligned} \mathbf{X} \;&=\mathbf{X}(\mathbf{q}, \mathbf{q}_x, ..., \partial_x, \partial_{xx}, ...; k) \\ \mathbf{T} \;&=\mathbf{T}(\mathbf{q}, \mathbf{q}_x, ..., \partial_x, \partial_{xx}, ...; k) \end{aligned}$$

on the potentials and a spectral parameter k, such that the overdetermined problem (*spectral problem*)

$$\Psi_x = \mathbf{X}\,\Psi \tag{2.2.2}$$

$$\Psi_t = \mathbf{T}\,\Psi \tag{2.2.3}$$

on the auxiliary eigenfunction Ψ, admits as compatibility condition $\Psi_{xt} = \Psi_{tx}$ the evolution equation. The linear problems defined by $\mathbf{X}$ and $\mathbf{T}$ are usually referred to as *scattering problem* and *auxiliary problem* respectively. Other requirements are that the spectral parameter to be time-independent (*isospectral*) and potentials go to zero as $x \to \infty$.

The IST can be broken into three steps:

- **the direct problem**: that is constructing the so called *scattering data* for the principal problem starting from the potentials $\mathbf{q}$ at the initial time, let us say $t_i = 0$;

- **time evolution**: determining the evolution of the scattering data by making use of the auxiliary problem;

- **the inverse problem**: reconstructing the potentials from the scattering data at final time $t_f = t$.

2.2.1 IST for the nonlinear Schröedinger equation

In this section we will apply the technique of the inverse scattering transform in order to find the one-soliton solution for the nonlinear Schöedinger equation

$$i\,q_t = q_{xx} + 2\mid q\mid^2 q \tag{2.2.1}$$

on the whole real line, i.e. $x \in \mathbb{R}$.

For the sake of simplicity, we will perform our analysis starting from the

well-known Zakharov-Shabat spectral problem, defined by

$$v_x = \begin{pmatrix} -ik & q \\ r & ik \end{pmatrix} v \tag{2.2.2}$$

and the following auxiliary problem

$$v_t = \begin{pmatrix} 2ik^2 + iqr & -2kq - iq_x \\ -2kr + ir_x r & -2ik^2 - iqr \end{pmatrix} v \tag{2.2.3}$$

where v is a two-component vector, k the spectral parameter and the q and r a couple of auxiliary potentials.

The compatibility condition provides the following system of equations

$$i\, q_t = q_{xx} - 2\, r\, q^2 \tag{2.2.4}$$

$$-i\, r_t = r_{xx} - 2\, q\, r^2, \tag{2.2.5}$$

which reduces to NLS through the reduction $r = -q^*$. Throughout the symbol "*" wil indicate the complex conjugate.

Let us firstly analyze the principal problem. Due to the vanishing conditions $q, r \to 0$ for $x \to \pm\infty$, the eigenfunctions of the scattering problem are asymptotic to the solutions of

$$v_x = \begin{pmatrix} -ik & 0 \\ 0 & ik \end{pmatrix} v \tag{2.2.6}$$

as $\mid x \mid \to \infty$.

Direct problem

The first step of IST consists in introducing a pair of bases for the spectral problem, defined by its asymptotic behaviour at $x \to -\infty$ (left basis) and $x \to +\infty$ (right basis) as

$$\phi(x,k) \sim \begin{pmatrix} 1 \\ 0 \end{pmatrix} e^{-ikx}, \qquad \bar{\phi}(x,k) \sim \begin{pmatrix} 0 \\ 1 \end{pmatrix} e^{ikx}, \quad x \to -\infty \tag{2.2.1}$$

$$\bar{\psi}(x,k) \sim \begin{pmatrix} 0 \\ 1 \end{pmatrix} e^{ikx}, \qquad \bar{\psi}(x,k) \sim \begin{pmatrix} 1 \\ 0 \end{pmatrix} e^{-ikx}, \quad x \to +\infty \tag{2.2.2}$$

These eigenfunctions are linearly independent due to the two following facts. For any two solutions $u(x,k)$ and $v(x,k)$ of (2.2.2) we have that

$$\frac{d}{dx}W(u,v) \;=\; 0 \tag{2.2.3}$$

being $W(u,v)$ the Wronskian of u and v. Further from asymptotics (2.2.6) one can see that

$$W\left(\phi,\bar{\phi}\right) \;=\; \lim_{x\to-\infty} W(\phi(x,k),\bar{\phi}(x,k)) = 1 \tag{2.2.4}$$

$$W\left(\psi,\bar{\psi}\right) \;=\; \lim_{x\to+\infty} W(\psi(x,k),\bar{\psi}(x,k)) = -1 \tag{2.2.5}$$

The two pairs of eigenfunctions are thus related, for every non singular k, by the following relations

$$\phi(x,k) \;=\; b(k)\psi(x,k) \;+\; a(k)\bar{\psi}(x,k) \tag{2.2.6}$$

$$\bar{\phi}(x,k) \;=\; \bar{a}(k)\psi(x,k) \;+\; \bar{b}(k)\bar{\psi}(x,k) \tag{2.2.7}$$

which define the scattering coefficients $a(k), \bar{a}(k), b(k)$ and $\bar{b}(k)$ of the problem. More remarkably, they can also be expressed in terms of Wronskians of the eigenfunctions

$$a(k) \;=\; W(\phi,\psi), \qquad \bar{a}(k) \;=\; -W(\bar{\phi},\bar{\psi}) \tag{2.2.8}$$

$$b(k) \;=\; -W(\phi,\bar{\psi}), \qquad \bar{b}(k) \;=\; W(\bar{\phi},\psi) \tag{2.2.9}$$

Together with these basis, it is then convenient to consider the set of Jost functions

$$M(x,k) \;=\; e^{ikx}\,\phi(x,k), \quad \bar{N}(x,k) \;=\; e^{ikx}\,\bar{\psi}(x,k) \tag{2.2.10}$$

$$N(x,k) \;=\; e^{-ikx}\,\psi(x,k), \quad \bar{M}(x,k) \;=\; e^{-ikx}\,\bar{\phi}(x,k) \tag{2.2.11}$$

which satisfy the following set of differential equations

$$\chi_x(x,k) \;=\; ik(\mathbf{J}+\mathbf{I})\chi(x,k) + (Q\chi)(x,k) \tag{2.2.12}$$

$$\tilde{\chi}_x(x,k) \;=\; ik(\mathbf{J}+\mathbf{I})\tilde{\chi}(x,k) + (Q\tilde{\chi})(x,k), \tag{2.2.13}$$

with constant boundary conditions

$$M(x,k) \to \begin{pmatrix} 1 \\ 0 \end{pmatrix}, \qquad \bar{M}(x,k) \to \begin{pmatrix} 0 \\ 1 \end{pmatrix}, \quad x \to -\infty \tag{2.2.14}$$

$$N(x,k) \to \begin{pmatrix} 0 \\ 1 \end{pmatrix}, \qquad \bar{N}(x,k) \to \begin{pmatrix} 1 \\ 0 \end{pmatrix}, \quad x \to +\infty. \tag{2.2.15}$$

where the quantity $\mathbf{J}$ and $\mathbf{Q}$ have been defined by

$$\mathbf{J} = \begin{pmatrix} -1 & 0 \\ 0 & 1 \end{pmatrix}, \qquad \mathbf{Q} = \begin{pmatrix} 0 & q \\ r & 0 \end{pmatrix}, \tag{2.2.16}$$

This formulation of the problem allows one to represent the Jost functions by means of the following Volterra integral equations

$$M(x,k) = \begin{pmatrix} 1 \\ 0 \end{pmatrix} + \int_{-\infty}^{+\infty} \mathbf{G}_+(x-x',k)(\mathbf{Q}M)(x',k)dx' \tag{2.2.17}$$

$$N(x,k) = \begin{pmatrix} 0 \\ 1 \end{pmatrix} + \int_{-\infty}^{+\infty} \tilde{\mathbf{G}}_+(x-x',k)(\mathbf{Q}N)(x',k)dx' \tag{2.2.18}$$

$$\bar{M}(x,k) = \begin{pmatrix} 0 \\ 1 \end{pmatrix} + \int_{-\infty}^{+\infty} \tilde{\mathbf{G}}_-(x-x',k)(\mathbf{Q}\bar{M})(x',k)dx' \tag{2.2.19}$$

$$\bar{N}(x,k) = \begin{pmatrix} 1 \\ 0 \end{pmatrix} + \int_{-\infty}^{+\infty} \mathbf{G}_-(x-x',k)(\mathbf{Q}\bar{N})(x',k)dx', \tag{2.2.20}$$

the matrix functions $\mathbf{G}$ and $\tilde{\mathbf{G}}$ being

$$\mathbf{G}_\pm = \pm\theta(\pm x) \begin{pmatrix} 1 & 0 \\ 0 & e^{2ikx} \end{pmatrix} \tag{2.2.21}$$

$$\tilde{\mathbf{G}}_\pm = \mp\theta(\mp x) \begin{pmatrix} e^{-2ikx} & 0 \\ 0 & 1 \end{pmatrix} \tag{2.2.22}$$

where $\theta(x)$ is the Heaviside function. Taking into account the summability of the potentials q, r it can be proved ([25]) that $M(x,k)$ and $N(x,k)$ are analytic functions in the upper-k plane and continuous up to the real axis,

while $\bar{M}(x,k)$ and $\bar{N}(x,k)$ are analytic functions of k in the lower-k plane and continuous up to the real axis. These properties ensures thus analyticity for the scattering coefficients $a(k)$ and $\bar{a}(k)$ for $\mathrm{Im}(k) > 0$ and $\mathrm{Im}(k) < 0$ respectively, due to the following integral relations

$$a(k) \;=\; 1 \;+\; \int_{-\infty}^{+\infty} q(x')M^{(2)}(x',k)dx' \tag{2.2.23}$$

$$b(k) \;=\; 1 \;+\; \int_{-\infty}^{+\infty} e^{-2ikx'} r(x')M^{(1)}(x',k)dx' \tag{2.2.24}$$

$$\bar{a}(k) \;=\; 1 \;+\; \int_{-\infty}^{+\infty} r(x')\bar{M}^{(1)}(x',k)dx' \tag{2.2.25}$$

$$\bar{b}(k) \;=\; 1 \;+\; \int_{-\infty}^{+\infty} e^{2ikx'} q(x')\bar{M}^{(2)}(x',k)dx' \tag{2.2.26}$$

The final step in the analysis of the scattering problem is to extract the so called proper eigenvalues of (2.2.2), that is the complex values of k ($\mathrm{Im}k \neq 0$) corresponding to bounded solutions v which vanish for large values of x. Because of (2.2.7) one can easily show that these values are the zeroes of $a(k)$ and $\bar{a}(k)$ in the upper and lower k-plane respectively. In correspondence of these critical values, from the relations between the scattering data and eigenfunctions, one can easily show that the following hold

$$\phi_j(x) \;=\; c_j\,\psi_j(x) \quad j = 1, ..., J \tag{2.2.27}$$

and

$$\bar{\phi}_j(x) \;=\; \bar{c}_j\,\bar{\psi}_j(x) \quad j = 1, ..., \bar{J} \tag{2.2.28}$$

where the coefficients c_j and $\bar{c}_j$ are the norming constants, while J and $\bar{J}$ denote the total number of zeroes for the coefficients $a(k)$ and $\bar{a}(k)$ in the upper and lower plane. In terms of Jost functions the norming constants are defined by

$$M_j \;=\; e^{2ik_jx}\,c_j\,N_j(x), \qquad \bar{M}_j \;=\; e^{-2i\bar{k}_jx}\,\bar{c}_j\,\bar{N}_j(x) \tag{2.2.29}$$

On the other hand the NLS corresponds to a symmetry reduction of the system (2.2.5) $r = -q^*$. Accordingly this symmetry in the potentials in-

duces a symmetry between the Jost functions analytic in the upper and lower complex plane, so that

$$\bar{\psi}(x,k) \;=\; \begin{pmatrix} \psi^{(2)}(x,k^*) \\ -\psi^{(1)}(x,k^*) \end{pmatrix}^*, \qquad \bar{\phi}(x,k) \;=\; \begin{pmatrix} -\phi^{(2)}(x,k^*) \\ \phi^{(1)}(x,k^*) \end{pmatrix}^* \tag{2.2.30}$$

$$\bar{N}(x,k) \;=\; \begin{pmatrix} N^{(2)}(x,k^*) \\ -N^{(1)}(x,k^*) \end{pmatrix}^*, \qquad \bar{M}(x,k) \;=\; \begin{pmatrix} -M^{(2)}(x,k^*) \\ M^{(1)}(x,k^*) \end{pmatrix}^* \tag{2.2.31}$$

and hence, due to (2.2.26), on the scattering coefficients

$$\bar{a}(k) \;=\; a^*(k^*) \tag{2.2.32}$$

$$\bar{b}(k) \;=\; -b^*(k^*) \tag{2.2.33}$$

From (2.2.33) it follows that k_j is zero of $a(k)$ if and only if k_j^* is a zero for $\bar{a}(k)$. Therefore $J = \bar{J}$ and

$$\bar{k}_j \;=\; k_j^*, \quad \bar{c}_j \;=\; -c_j^*, \quad j = 1, ..., J. \tag{2.2.34}$$

Evolution of scattering data

In order to get the time evolution of the scattering data, we can look for solutions of the auxiliary problem in the form

$$\Phi(x,t) \;=\; e^{A_\infty t}\phi(x,t), \quad \bar{\Phi}(x,t) \;=\; e^{-A_\infty t}\bar{\phi}(x,t) \tag{2.2.1}$$

$$\Psi(x,t) \;=\; e^{-A_\infty t}\psi(x,t), \quad \bar{\Psi}(x,t) \;=\; e^{A_\infty t}\bar{\psi}(x,t) \tag{2.2.2}$$

where $A_\infty = 2ik^2$. Then the evolution equations become

$$\partial_t\,\phi \;=\; \begin{pmatrix} A - A_\infty & B \\ C & -A - A_\infty \end{pmatrix} \phi \tag{2.2.3}$$

$$\partial_t\,\bar{\phi} \;=\; \begin{pmatrix} A + A_\infty & B \\ C & -A + A_\infty \end{pmatrix} \phi \tag{2.2.4}$$

being A, B, C the corresponding entries of temporal Lax operator. By taking into account (2.2.7) and letting $x \to +\infty$ one finally gets

$$\partial_t\, a(k,t) = 0, \qquad \partial_t\, \bar{a}(k,t) = 0 \tag{2.2.5}$$

$$\partial_t\, b(k,t) = -2A_\infty\, b(k), \qquad \partial_t\, \bar{b}(k,t) = 2A_\infty\, \bar{b}(k) \tag{2.2.6}$$

whose solution is

$$a(k,t) \;=\; a(k,0), \qquad \bar{a}(k,t) \;=\; \bar{a}(k,0) \tag{2.2.7}$$

$$b(k,t) \;=\; e^{-4ik^2t}\, b(k,0), \qquad \bar{b}(k,t) \;=\; e^{4ik^2t}\, \bar{b}(k,0). \tag{2.2.8}$$

On the other hand, by introducing the reflection coefficients $\rho(k,t) = b(k,t)/a(k,t)$ and the modified norming constants $C_j = c_j/a'(k_j)$, we also have

$$\rho(k,t) \;=\; e^{-4ik^2t}\, b(k,0), \qquad \bar{\rho}(k,t) \;=\; e^{4ik^2t}\, \bar{b}(k,0) \tag{2.2.9}$$

$$C_j(t) \;=\; C_j(0)\, e^{-4ik^2t}, \qquad \bar{C}_j(t) \;=\; \bar{C}_j(0)\, e^{4ik^2t}. \tag{2.2.10}$$

Inverse scattering problem

The final step of the IST consists in reversing the one-to-one map which, starting from the potentials, allow to build up the Jost functions of the principal problem and the corresponding scattering data.

Due to the analyticity of $N(x,k)$ and $\bar{N}(x,k)$ in the regions $\mathrm{Im}k > 0$ and $\mathrm{Im}k < 0$, the functions $\mu(x,k)$ and $\bar{\mu}(x,k)$ defined by

$$\mu(x,k) \;=\; M(x,k)\, a^{-1}(k), \quad \bar{\mu}(x,k) \;=\; \bar{M}(x,k)\, \bar{a}^{-1}(k). \tag{2.2.1}$$

are meromorphic in the upper and lower complex plane, respectively. Therefore, the inverse problem consists in finding out the unknown sectionally meromorphic functions satisfying the following "scattering" relations

$$\mu(x,k) \;=\; \bar{N}(x,k) + \rho(k) e^{2ikx}\, N(x,k) \tag{2.2.2}$$

$$\bar{\mu}(x,k) \;=\; N(x,k) + \bar{\rho}(k) e^{-2ikx}\, \bar{N}(x,k) \tag{2.2.3}$$

Let us assume that the potential is such that $a(k)$ have a finite number of simple zeroes (soliton solutions for NLS) and that $a(\xi) \neq 0$ for any $\xi \in \mathbb{R}$. By applying the projection operators P^- and P^+, defined as

$$P^{\pm}(f)(k) \;=\; \frac{1}{2\pi i}\int_{-\infty}^{+\infty} \frac{f(\zeta)}{\zeta-(k\pm i0)}d\zeta \tag{2.2.4}$$

to (2.2.3) and (2.2.3) respectively, it can be proved that

$$\bar{N}(x,k) \;=\; \begin{pmatrix} 1 \\ 0 \end{pmatrix} + \sum_{j=1}^{J} \frac{C_j\, e^{2ik_j x}\, N_j(x)}{k-k_j} + \frac{1}{2\pi i}\int_{-\infty}^{+\infty} \frac{\rho(\xi) e^{2i\xi x} N(x,\xi)}{\xi-(k-i0)}d\xi \tag{2.2.5}$$

$$N(x,k) \;=\; \begin{pmatrix} 0 \\ 1 \end{pmatrix} + \sum_{j=1}^{\bar{J}} \frac{\bar{C}_j\, e^{-2i\bar{k}_j x}\, \bar{N}_j(x)}{k-\bar{k}_j} - \frac{1}{2\pi i}\int_{-\infty}^{+\infty} \frac{\bar{\rho}(\xi) e^{-2i\xi x} \bar{N}(x,\xi)}{\xi-(k+i0)}d\xi \tag{2.2.6}$$

By evaluating now the equations (2.2.6) at $k=\bar{k}_l$ for $l=1,...,\bar{J}$ and (2.2.6) at $k=k_j$ for $j=1,...,J$ we have

$$\bar{N}_l(x) \;=\; \begin{pmatrix} 1 \\ 0 \end{pmatrix} + \sum_{j=1}^{J} \frac{C_j\, e^{2ik_j x}\, N_j(x)}{\bar{k}_l-k_j} + \frac{1}{2\pi i}\int_{-\infty}^{+\infty} \frac{\rho(\xi) e^{2i\xi x} N(x,\xi)}{\xi-\bar{k}_l}d\xi \tag{2.2.7}$$

$$N_j(x,k) \;=\; \begin{pmatrix} 0 \\ 1 \end{pmatrix} + \sum_{m=1}^{\bar{J}} \frac{\bar{C}_m\, e^{-2i\bar{k}_m x}\, \bar{N}_m(x)}{k_j-\bar{k}_m} - \frac{1}{2\pi i}\int_{-\infty}^{+\infty} \frac{\bar{\rho}(\xi) e^{-2i\xi x} \bar{N}(x,\xi)}{\xi-k_m}d\xi \tag{2.2.8}$$

which is a linear algebraic-integral system of equations which, in principle, solve the inverse problem for the eigenfunctions $N(x,k)$ and $\bar{N}(x,k)$. By performing the asymptotic expansion of (2.2.8-2.2.8) to the expansions of (2.2.20) we obtain the

$$r(x) \;=\; -2i\sum_{j=1}^{J} e^{2ik_j x}\, C_j N_j^{(2)}(x) + \frac{1}{\pi}\int_{-\infty}^{+\infty} \rho(\xi) e^{2i\xi x} N^{(2)}(x,\xi)d\xi \tag{2.2.9}$$

$$q(x) \;=\; 2i\sum_{j=1}^{\bar{J}} e^{-2i\bar{k}_j x}\, \bar{C}_j \bar{N}_j^{(1)}(x) + \frac{1}{\pi}\int_{-\infty}^{+\infty} \bar{\rho}(\xi) e^{-2i\xi x} \bar{N}^{(1)}(x,\xi)d\xi, \tag{2.2.10}$$

which reconstruct the potentials.

2.2.2 Soliton solutions for the NLS

In order to recover the one-soliton solution we have to impose that the $\rho(\xi) = 0$ for every $\xi \in \mathbb{R}$, in such a way the algebraic-integral system (2.2.8-2.2.8) reduces to the linear algebraic system

$$\bar{N}_l(x) \;=\; \begin{pmatrix} 1 \\ 0 \end{pmatrix} + \sum_{j=1}^{J} \frac{C_j\, e^{2ik_j x}\, N_j(x)}{\bar{k}_l - k_j} \tag{2.2.1}$$

$$N_j(x,k) \;=\; \begin{pmatrix} 0 \\ 1 \end{pmatrix} + \sum_{m=1}^{\bar{J}} \frac{\bar{C}_m\, e^{-2i\bar{k}_m x}\, \bar{N}_m(x)}{k_j - \bar{k}_m} \tag{2.2.2}$$

By fixing $J = \bar{J} = 1$ and imposing the reduction $r = -q^*$, we get

$$N_1^{(1)}(x) \;=\; -\frac{C_1^*}{k_1 - \bar{k}_1^*}\, e^{-2ik_1^* x} \left(1 - \frac{\mid C_1 \mid^2 e^{2i(k_1 - k_1^*)x}}{(k_1 - k_1^*)^2}\right)^{-1} \tag{2.2.3}$$

$$N_1^{(2)}(x) \;=\; \left(1 - \frac{\mid C_1 \mid^2 e^{2i(k_1 - k_1^*)x}}{(k_1 - k_1^*)^2}\right)^{-1} \tag{2.2.4}$$

and finally from (2.2.10) the one-soliton solution

$$q(x) \;=\; -2i\eta \frac{C_1^*}{\mid C_1 \mid} e^{-2i\xi x} \mathrm{sech}(2\eta x - 2\delta) \tag{2.2.5}$$

where

$$k_1 \;=\; \xi + i\,\eta, \qquad e^{2\delta} \;=\; \frac{\mid C_1 \mid}{2\eta} \tag{2.2.6}$$

Including then the time dependence of C_1 given by (2.2.10) the moving one-soliton solution of the focusing NLS,

$$q(x,t) \;=\; 2\eta e^{-2i\xi x + 4i(\xi^2 - \eta^2)t - i(\psi_0 + \pi/2)} \mathrm{sech}(2\eta x \;-\; 8\xi\eta t - 2\delta_0) \tag{2.2.7}$$

with

$$e^{2\delta_0} \;=\; \frac{\mid C_1(0) \mid}{2\eta}, \qquad \psi_0 \;=\; arg C_1(0). \tag{2.2.8}$$

Chapter 3

One-Dimensional Bose Gases with N-Body Attractive Interactions

As discussed in Chapter 1 , the technique of Feshbach resonances allows for a change of the sign of the scattering length: by switching from repulsion to attraction, i.e. from positive to negative scattering length, the homogeneous 1-D Gross-Pitaevskii equation (GPE) admits a solution corresponding to a localized wave-function (bright soliton) [25]. Bright matter-wave solitons have been created both in Bose-Einstein condensates of ^{7}Li [35, 37] and ^{85}Rb atoms [55]. Several localized states have also been produced in quasi-one-dimensional geometries [56].

With attractive two-body interactions, a crucial role is played both by the dimension of the system and the trapping potential. In three dimensions, for instance, homogeneous attractive bosons are unstable against the collapse, but the presence of an external harmonic trap can stabilize them: the critical value of the interaction coupling that gives rise to the collapse can be obtained from the GPE [2, 3], and the critical particle number is given

by $\sim \mathcal{N}_T \mid a \mid /a_{osc}$ where $\mathcal{N}_T$ is the total number of particles, $a < 0$ is the scattering length and a_{osc} is the harmonic oscillator length [33, 32, 57, 47]. In the one-dimensional case, the bright soliton solution is the ground state of the homogeneous GPE with negative scattering length. Furthermore, the GPE ground state energy is in agreement, in the thermodynamic limit, with the ground state energy obtained by Bethe ansatz for the attractive one-dimensional Bose gas [58] (see more in section 3.1).

In this Chapter, motivated by the recent papers [19, 21] in which different schemes have been proposed to realize effective tunable three-body interactions, we consider an attractive three-body contact potential and, more generally, a N-body contact interaction. We consider the limit of large number of particles, $\mathcal{N}_T >> 1$, with the constraint $c\mathcal{N}_T^{(N-1)} = const$ (c being the strength of the N-body interactions) so that the energy per particle is finite. Since no Bethe solution is known in the general case of N-body interaction, we employ an Hartree approximation to study the problem in the limit mentioned above. This means that the ground state energy is estimated by using the bright soliton solution of a generalized mean-field GPE equation. As we will show, the $N = 3$ is a special case: for this value, in fact, a localized soliton wavefunction exists only for a critical value of the interaction strength and has an infinite degeneracy. The stabilization of this bound state can be cured by putting the system in an external harmonic trap. The variational approach, that we will also employ, reveals the tendency of the higher body interactions to become more unstable in higher dimensions. It is worth stressing that the case we are considering does not consist of a N-body interaction added to the 2-body interaction of the Bose gas: we are interested, in fact, to the effect of the N-body in its own, since the coefficient of the two-body interaction can be tuned to be zero [19].

The plan of the chapter is the following: in section 3.1 we introduce the Hamiltonian corresponding to N-body contact attractive interactions

and we write the (mean-field) generalized GPE. The familiar case $N = 2$ is briefly recalled. In section 3.2 the bright soliton solution for the homogeneous limit is obtained by using a mechanical analogy with a fictitious particle moving in a potential, and its properties are investigated. The comparison with the numerical results confirms that for $N \leq 3$ this is the ground state of the generalized GPE, as expected. The ground state energy by varying N is also determined. In section 3.3 we consider the effect of an harmonic trap: using a variational ansatz for the ground state we determine the critical value of the interaction needed to stabilize the bound state.

3.1 N-body attractive contact interactions

The general quantum Hamiltonian for an homogeneous one-dimensional Bose gas with N-body interactions $V(x_1, \cdots, x_N)$ is

$$\hat{H} = \int dx \hat{\Psi}^\dagger(x) \left(-\frac{\hbar^2}{2m} \frac{\partial^2}{\partial x^2} \right) \hat{\Psi}(x) \tag{3.1.1}$$
$$+ \frac{1}{N!} \int dx_1 \cdots dx_N \hat{\Psi}^\dagger(x_1) \cdots \hat{\Psi}^\dagger(x_N) V(x_1, \cdots, x_N) \hat{\Psi}(x_N) \cdots \hat{\Psi}(x_1) \ ,$$

where $\hat{\Psi}(x)$ is the bosonic field operator. Let us note that the Lieb-Liniger model for the interacting one-dimensional Bose gas [10] is recovered for $N = 2$ and $V(x_1, x_2) = V_0 \, \delta(x_1 - x_2)$: where V_0 positive (negative) corresponds to repulsion (attraction) between the bosons. The low-energy properties of the Lieb-Liniger model can be studied by the Luttinger liquid effective description [59] obtained by bosonization [60] (a general discussion of the correlation functions is presented in [61]).

For N-body attractive contact interactions we set

$$V(x_1, \cdots, x_N) = -c \prod_{i=1}^{N-1} \delta(x_i - x_{i+1}) \quad c > 0 \tag{3.1.2}$$

so that the Hamiltonian (3.1.1) reads

$$\hat{H} = \int dx \hat{\Psi}^\dagger(x) \left(-\frac{\hbar^2}{2m} \frac{\partial^2}{\partial x^2} \right) \hat{\Psi}(x) - \frac{c}{N!} \int dx \left[\hat{\Psi}^\dagger(x) \right]^N \left[\hat{\Psi}(x) \right]^N \quad . \tag{3.1.3}$$

In the Heisenberg representation, the equation of motion for the field operator is given by

$$i\hbar \frac{\partial \hat{\Psi}}{\partial t} = \left[\hat{\Psi}, \hat{H} \right] = -\frac{\hbar^2}{2m} \frac{\partial^2}{\partial x^2} \hat{\Psi} - c \left(\hat{\Psi}^\dagger \right)^{N-1} \left(\hat{\Psi} \right)^{N-1} \hat{\Psi} \quad . \tag{3.1.4}$$

As we have seen in the previous chapter, the Lieb-Liniger model ($N = 2$) is integrable and its ground state energy E reduces, for large L, to the following expression [62]

$$\frac{E}{\mathcal{N}_T} = -\frac{mc^2 \left(\mathcal{N}_T^2 - 1 \right)}{24\hbar^2} \quad , \tag{3.1.5}$$

where $\mathcal{N}_T$ is the total number of particles. For large $\mathcal{N}_T$, from (3.1.5) it follows that one has to keep the product $c\mathcal{N}_T = const$ in order to have a finite ground state energy per particle. Using the integrability of the $N = 2$ model, the correlation functions of the one-dimensional Bose gas at zero temperature were recently calculated both in attractive [65] and repulsive regime [63, 64].

For the three-body problem ($N = 3$), no Bethe ansatz solution is available, except for a more complicate double-δ function Bose gas which can be mapped in a one-dimensional anyon gas [66]. Hence, to estimate the ground state energy E we propose here to employ a mean-field (Hartree) approach: in this approach, the ground state energy is given in terms of the ground state energy of a generalized GPE. The same procedure will be employed for other values of N.

Before starting the discussion of the general N-body case, let us briefly remind how this task can be successfully performed for $N = 2$ [58]. First of all, in the mean-field approximation the ground state wavefunction is

written as

$$\psi_{GS}(x_1, \cdots, x_{\mathcal{N}_T}) \propto \prod_{i=1}^{\mathcal{N}_T} \psi_0(x_i) \ , \tag{3.1.6}$$

where the function $\psi_0(x)$ is the ground state of the time-independent homogeneous GPE, i.e. the nonlinear Schrödinger equation (NLSE), given by

$$-\frac{\hbar^2}{2m}\frac{\partial^2}{\partial x^2}\psi_0 - c \mid \psi_0 \mid^2 \psi_0 \ = \ \mu\psi_0 \ , \tag{3.1.7}$$

where μ is the chemical potential and the normalization is given by

$$\int dx \mid \psi_0 \mid^2 = \mathcal{N}_T. \tag{3.1.8}$$

The energy is expressed as

$$E_{GP} \ = \ \int dx \, \psi_0^*(x) \left[-\frac{\hbar^2}{2m}\frac{\partial^2}{\partial x^2} - \frac{c}{2} \mid \psi_0(x) \mid^2 \right] \psi_0(x) \ . \tag{3.1.9}$$

The static bright soliton solution of (3.1.7) is given by

$$\psi_0(x) \ = \ \sqrt{\mathcal{N}_T}\frac{\mathcal{N}}{\cosh(kx)} \ , \tag{3.1.10}$$

with

$$k = \frac{mc\mathcal{N}_T}{2\hbar^2}, \qquad \mathcal{N} = \frac{\sqrt{mc\mathcal{N}_T/\hbar^2}}{2}. \tag{3.1.11}$$

Substituting this expression in (3.1.9) one gets

$$\frac{E_{GP}}{\mathcal{N}_T} \ = \ -\frac{mc^2\mathcal{N}_T^2}{24\hbar^2} \ , \tag{3.1.12}$$

i.e., the exact result (3.1.5) up to a factor $\propto 1/\mathcal{N}_T^2$. A comment is in order: in the homogeneous one-dimensional interacting case there is, strictly speaking, no condensate. However the condition $c\mathcal{N}_T = const$ implies that, for large $\mathcal{N}_T$, the coupling constant should scale to zero, $c \to 0$: hence, we are in a weak coupling regime where the mean-field GPE is expected to give reasonable results. In a similar way, for $c < 0$ (repulsive interaction) the comparison between the exact and the GPE ground state energy shows

that the latter gives the correct behaviour for $c \to 0$ while the Bogoliubov approximation gives the exact first-order corrections for small $\mid c \mid$ [10].

Based on the analysis above, for general N and in the limit $c \to 0$ we expect that a reasonable description of both the ground state properties and the low-energy dynamics is given by the mean-field generalized homogeneous GPE

$$i\hbar\frac{\partial\psi(x,t)}{\partial t} \;=\; \left(-\frac{\hbar^2}{2m}\frac{\partial^2}{\partial x^2} - c|\psi(x,t)|^{\alpha}\right)\psi(x,t) \;\;, \tag{3.1.13}$$

where the nonlinearity degree α of the "power-law" nonlinear Schrödinger equation (PL-NLSE) (3.1.13) is related to N by

$$N \equiv \frac{\alpha}{2} + 1 \;\;. \tag{3.1.14}$$

The mean-field ground state is given by the time-independent PL-NLSE equation

$$\left(-\frac{\hbar^2}{2m}\frac{\partial^2}{\partial x^2} - c|\psi_0(x)|^{\alpha}\right)\psi_0(x) \;=\; \mu\psi_0(x) \;\;, \tag{3.1.15}$$

where, as before, μ is chemical potential and ψ_0 is normalized to the total number of particles $\mathcal{N}_T$, i.e. $\int dx|\psi_0(x)|^2 = \mathcal{N}_T$. eqn. (3.1.13) is a particular case of the following generalized NLSE

$$i\hbar\frac{\partial\psi(x,t)}{\partial t} \;=\; \left(-\frac{\hbar^2}{2m}\frac{\partial^2}{\partial x^2} - \mathcal{F}\left(\mid \psi(x,t) \mid\right)\right)\psi(x,t) \;\;, \tag{3.1.16}$$

where $\mathcal{F}\left(\mid \psi \mid\right)$ is a general function (see more references in the reviews [67, 68]). Eqn. (3.1.13) corresponds to a power-law dependence $\mathcal{F} \sim \mid \psi \mid^{\alpha}$, and it is used in several physical contexts, including semiconductors [69] and nonlinear optics [24, 70, 71], where it describes pulse propagation in optical materials having a power law dependence of the refractive index on intensity. In the present context of ultracold bosonic gases, the nonlinearity degree α depends through eqn. (3.1.14) on the number of bodies which interacts between themselves.

With $N \geq 2$ integer, α is an even integer; however, in eqn. (3.1.15) α can take any real positive value and, in the following, we will consider this general case. In this respect let us remark that the axial dynamics of a Bose-Einstein condensate induced by an external potential with cylindrical symmetry in the transverse directions can be studied by introducing an effective one-dimensional GPE equation with $\alpha = 1$ [30] and that for Bose-Einstein condensates in one-dimensional optical lattices the effective equation has a value of α that depends on the details of the trapping potentials and it is, in general, a non-integer value [72].

3.2 Ground state of the generalized nonlinear Schrödinger equation

In the following we will study the attractive N-body problem in the thermodynamic limit, defined by $\mathcal{N}_T \to \infty$, with the product $G = c\mathcal{N}_T^{\alpha/2}$ kept fixed. This will ensure the energy per particle of the PL-NLSE bright soliton to be finite. In dimensionless units, rescaling the wave function $\psi_0 \to \sqrt{\mathcal{N}_T}\psi_0$, eqn. (3.1.15) reads

$$\left(-\frac{1}{2}\frac{\partial^2}{\partial x^2} - g|\psi_0(x)|^\alpha\right)\psi_0(x) \;=\; \tilde{\mu}\psi_0(x) \;\;, \tag{3.2.17}$$

where g and $\tilde{\mu}$ are the dimensionless versions of c and μ, respectively (by choosing ℓ as unit length, one has $\tilde{\mu} = \mu\ell^2 m\mu/\hbar^2$ and $g = Gm\ell^{2-\alpha/2}/\hbar^2$). For the ground state of this equation we look for a real solution, with the normalization condition

$$\int_{-\infty}^{\infty} \psi_0^2(x)\, dx \;=\; 1 \;\;. \tag{3.2.18}$$

Obviously, once a static solution $\psi_0(x)$ of eqn. (3.2.17) has been found, the corresponding soliton wave solution with velocity v is given by

$$\psi_0(x,t) \;=\; \psi_0(x - vt)\, e^{-i(\tilde{\mu}t - vx + v^2 t/2)} \;\;. \tag{3.2.19}$$

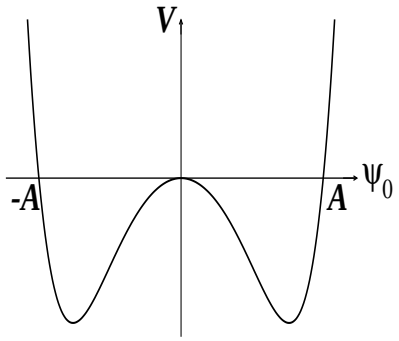

Figure 3.1: Typical shape of the potential $V(\psi_0)$ for negative values of $\tilde{\mu}$. $\pm A$ are the inversion points of the motion.

The real solution of eqn. (3.2.17) can be found by using a mechanical analogy. In fact, interpreting x as the time variable and $\psi_0(x)$ as the coordinate of a fictitious particle, eqn. (3.2.17) formally corresponds to the Newton's equation of motion of this particle (of mass $M = 1/2$), subjected to the force

$$F = -\tilde{\mu}\psi_0 - g\psi_0^{\alpha+1} \ . \tag{3.2.20}$$

This force can be derived by the potential

$$V(\psi_0) = \frac{\tilde{\mu}}{2}\psi_0^2 + \frac{g}{\alpha+2}\psi_0^{\alpha+2} \ . \tag{3.2.21}$$

As any motion of a particle in a potential, this is accompanied by the integral of motion that corresponds to its mechanical energy

$$\mathcal{H} = \frac{M}{2}\left(\frac{d\psi_0}{dx}\right)^2 + V(\psi_0) = \text{const} \ . \tag{3.2.22}$$

Following this mechanical analogy and looking at the typical shape of the potential (see the plot in Fig. 3.1), it is straightforward to realize that non-trivial motions can take place only if $\tilde{\mu} < 0$.

Notice that a solution is always given by the equilibrium configuration

of the potential (3.2.21)

$$\psi_0(x) = \left(\frac{-\tilde{\mu}}{g}\right)^{1/\alpha} \quad . \tag{3.2.23}$$

Since this solution can be normalized only on a finite volume L, from the normalization condition (3.2.18) we then recover the following relation between the chemical potential and the volume

$$\tilde{\mu} = -gL^{-\alpha/2}. \tag{3.2.24}$$

Hence the constant solution simply reads

$$\psi_0 = \frac{1}{\sqrt{L}} \ . \tag{3.2.25}$$

In order to determine the ground state, we are going to compare the GPE energy of the above constant solution with the one of a localized wavefunction.

Taking the mechanical analogy, we look for a solution whose asymptotics behaviour reproduces a finite value for the auxiliary Hamiltonian $\mathcal{H}$. By imposing that both the solution $\psi_0(x)$ and its derivative $\frac{d\psi_0}{dx}(x)$ vanish as $x \to \pm\infty$ (localized solution), we get that $\mathcal{H}$ is identically zero (notice that this value is *not* the GPE energy).

The interpretation is that, the fictitious particle takes off from the origin at $x = -\infty$, moving to the right (or, equivalently to the left, since the original equation is invariant under $\psi_0(x) \to -\psi_0(x)$), until it reaches the inversion point A at the time $x = 0$. Once the particle arrives in A, it inverts its motion and comes back to the origin with a vanishing velocity. The important point of this picture is that A coincides with the maximum amplitude of the bright soliton solution. An additional remarks is now in orded: the kind of motion we have just described occurs for any potential with the shape shown in Fig. 3.1. Thus, in order to keep a physical meaning to the wavefunction, a further constraint (3.2.18) has to be imposed. This

condition can be fulfilled only for a particular shape of the potential, i.e. for a particular combination of the parameters $\tilde{\mu}$ and g: *it is as if the solution is looking for its proper potential.*

In the following, it is convenient to introduce the quantities

$$a^2 \equiv -\frac{\tilde{\mu}(\alpha+2)}{2g} > 0 \quad , \quad b \equiv \sqrt{\frac{4g}{\alpha+2}} \quad , \quad \gamma \equiv \frac{2}{\alpha} \ . \tag{3.2.26}$$

Using the integral of motion $\mathcal{H}$, for generic values of $\tilde{\mu}$, g and α (with $\tilde{\mu} < 0$, $g > 0$ and $\alpha > 0$) the solution is given by a quadrature

$$\int_A^{\psi_0(x)} \frac{dq}{\sqrt{a^2q^2 - q^{\alpha+2}}} \ = \ b \int_0^x d\tau \ , \tag{3.2.27}$$

where $A = a^\gamma$ is the inversion point reached by the particle at the "time" $x = 0$. Using the exact expression of the integral of the left hand side [74]

$$\int_A^{\psi_0(x)} \frac{dq}{\sqrt{a^2q^2 - q^{\alpha+2}}} \ = \ -\frac{1}{a\alpha} \ln \left[\frac{a + \sqrt{a^2 - \psi_0^\alpha(t)}}{a - \sqrt{a^2 - \psi_0^\alpha(t)}} \right] \ , \tag{3.2.28}$$

one gets

$$\psi_0(x) \ = \ \frac{A}{\cosh^\gamma \left(\frac{\alpha}{2} \sqrt{-2\tilde{\mu}}\, x \right)} \ . \tag{3.2.29}$$

By imposing now the normalization condition (3.2.18) to the solution (3.2.29): we finally get the relation between $\tilde{\mu}$ and g, which is equivalent to fix the shape of the potential

$$(-\tilde{\mu})^{\frac{4-\alpha}{2\alpha}} = g^{2/\alpha} \left(\frac{2}{\alpha+2} \right)^{2/\alpha} \frac{\alpha \Gamma(2/\alpha + 1/2)}{\sqrt{2\pi}\Gamma(2/\alpha)} \ . \tag{3.2.30}$$

When $\alpha \neq 4$, we can use this equation to express $\tilde{\mu}$ as a function of g and, in particular, to write the normalization A as

$$A \ = \ \left(\sqrt{\frac{2g}{\pi\gamma(\gamma+1)}} \frac{\Gamma(\gamma+1/2)}{\Gamma(\gamma)} \right)^{\frac{2}{4-\alpha}} \ . \tag{3.2.31}$$

In Fig. 3.2 we plot the soliton solution (3.2.29) for different values of α at $g = 1$.

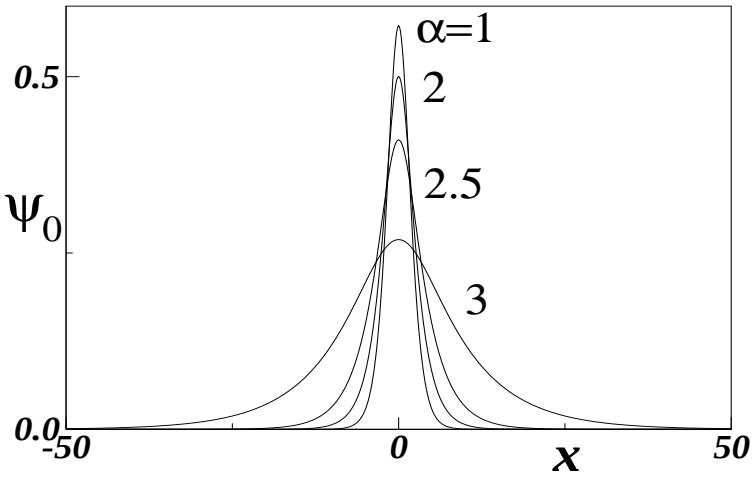

Figure 3.2: Ground state wavefunctions of the PL-NLSE (3.2.17) for $\alpha = 1, 2, 2.5, 3$ (dimensionless units are used with $g = 1$).

Reamarkably enough, when $\alpha = 4$, eqn. (3.2.30) leaves $\tilde{\mu}$ undetermined: this means that the corresponding wavefunction

$$\psi_0(x) \;=\; \left(\frac{\sqrt{-3\tilde{\mu}/g}}{\cosh(2\sqrt{-2\tilde{\mu}}\, x)} \right)^{1/2} \tag{3.2.32}$$

is solution of the nonlinear Schrödinger equation (3.2.17) for *every* $\tilde{\mu}$. In this case, however, only a particular value of g, given by

$$g^* \;=\; \frac{3\pi^2}{8} \;, \tag{3.2.33}$$

guarantees its correct normalization (3.2.18). Expressed in more physical terms, the attractive 3-body interaction has the peculiarity that one can arbitrarily vary the chemical potential provided that the coupling constant be fine-tuned to the critical value g^*: increasing or decreasing (in modulus) the chemical potential simply results, in this case, in shrinking or enlarging the shape of the soliton. This is shown in Fig. 3.3 where the wavefunction (3.2.32) is plotted for two different values of $\tilde{\mu}$: in the inset we plot the

corresponding potential (3.2.21), showing a larger (smaller) inversion point corresponding to the smaller (larger) width.

The fact that $\tilde{\mu}$ is undetermined and the soliton can arbitrarily change its shape does not imply that the GPE energy is undetermined: in fact, the explicit computation of the next subsection shows that, in this case, the energy does not depend on the value of $\tilde{\mu}$. Then, for $N = 3$ and $g = g^*$, an infinite degeneracy parametrized by the chemical potential $\tilde{\mu} < 0$ occurs.

In Fig. 3.4(a)-(b) we plot the chemical potential $\tilde{\mu}$ for two different values of g, one smaller than g^* and the other larger: it is seen that for $g < g^*$ ($g > g^*$), then $\tilde{\mu} \to 0$ ($\tilde{\mu} \to -\infty$) for $\alpha \to 4^-$, while $\tilde{\mu} \to \infty$ ($\tilde{\mu} \to 0$) for $\alpha \to 4^+$. The singular nature of the 3-body interaction can then be recovered by studying the limit $\alpha \to 4$ of the formulas (3.2.29), (3.2.30), (3.2.31) given above: for $\alpha \to 4^-$, if $g = g^*$ the normalization A goes to 1, while if $g < g^*$, $A \to 0$ and $\tilde{\mu} \to 0$ (i.e. we have a non-localized solution) whereas if $g > g^*$, both A and $\tilde{\mu}$ diverge, i.e. the wavefunction collapses to the origin.

It is worth to mention that a singular behavior of the nonlinear Schrödinger equation, corresponding to a self-focusing singularity present at the value $\alpha = 4$ [73], has also been observed in the dynamical blowing up of the moving wave-packets of this equation [75]. In the present application, this instability means that the local 3-body attractive interactions cannot sustain a bound state unless there is a fine tuning of the interaction. In the next section we will show how an external trap can help to stabilize the bound state for a generic value of the coupling.

To better understand the behaviour of the solution $\psi_0(x)$ as a function of α, let us study in which way the soliton width σ_α defined as usual

$$\sigma_\alpha^2 = \int dx x^2 \psi_0^2(x) \tag{3.2.34}$$

depends on the microscopic interactions. Inserting (3.2.32) in (3.2.34), one

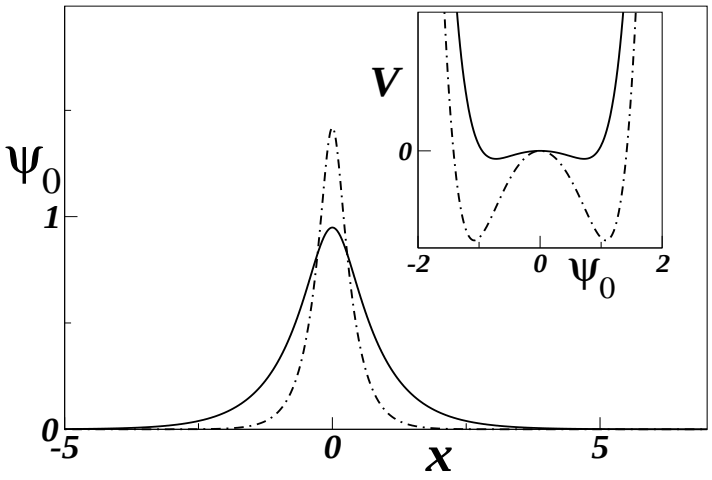

Figure 3.3: Wavefunction (3.2.32) for $N = 3$ and $g = g^*$ plotted for $\tilde{\mu} = -1$ (solid line) and $\tilde{\mu} = -5$ (dot-dashed line). Inset: corresponding potential (3.2.21) for $\tilde{\mu} = -1$ (solid line) and $\tilde{\mu} = -5$ (dot-dashed line).

gets

$$\sigma_\alpha^2 = \frac{\Gamma(\gamma + 1/2)}{\pi\Gamma(\gamma)} \cdot \frac{\gamma(\gamma+1)}{2A^\alpha} \cdot \mathcal{I}_\alpha \ , \tag{3.2.35}$$

where

$$\mathcal{I}_\gamma = \int dX \, \frac{X^2}{\cosh^{2\gamma}(X)}, \qquad \gamma > 0. \tag{3.2.36}$$

One finds $\sigma_2^2(g) = \pi^2/3g \approx 3.28/g$ and $\sigma_1^2(g) = (\pi^2 - 6)/(12g)^{1/3} \approx 1.69/g^{1/3}$. For large α one has $\sigma_\alpha^2 \to g/2$, while, of course, $\sigma_\alpha^2 \to \infty$ for $\alpha \to 0$ (no localized soliton without interaction).

For $g < g^*$, from eqn. (3.2.35) one sees that for $\alpha \to 4^-$, $\sigma_\alpha \to \infty$, while for $\alpha \to 4^+$, $\sigma_\alpha \to 0$. In Fig. 3.5 we report, for $g = 1 < g^*$, the analytical values of the width σ_α^2 and their numerical estimates obtained from the PL-NLSE. A divergence is observed for $\alpha \to 4^-$, corresponding to the 3-body attraction: the bright soliton becomes larger and larger getting close to $\alpha = 4$, while for α slightly larger than 4 the soliton becomes extremely

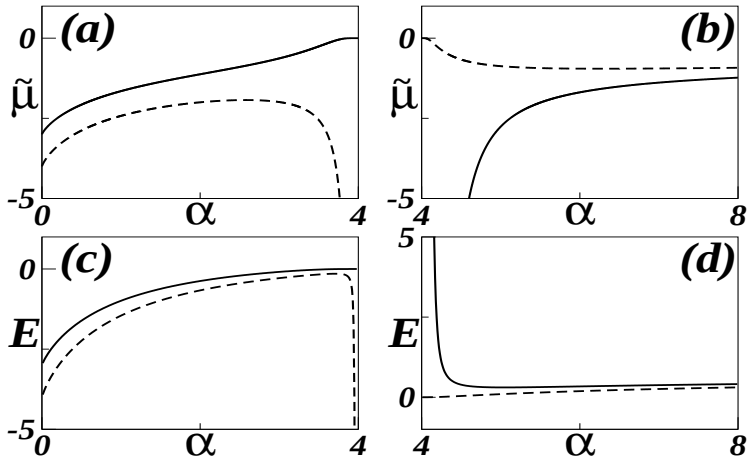

Figure 3.4: (a)-(c) Chemical potential and energy (in dimensionless units) of the bright soliton solution (3.2.29) for $g = 3 < g^*$ (solid line) and $g = 4 > g^*$ (dashed line) for $\alpha < 4$ - (b)-(d) chemical potential and energy for $g = 3$ (solid line) and $g = 4$ (dashed line) for $\alpha > 4$.

narrow. This means that there is a collapse of the solution (3.2.29) going to $\alpha = 4$ from large values of α.

On the other hand, for $g > g^*$, then for $\alpha \to 4^-$, $\sigma_\alpha \to 0$, while for $\alpha \to 4^+$, $\sigma_\alpha \to \infty$. It should be stressed that, for $\alpha > 4$, although (3.2.29) is a solution of the PL-NLSE (3.2.17), it is no longer its ground state: the divergence of σ_α for $\alpha \to 4^-$ is a signature of the disappearance of the bound state due to the 3-body interaction.

To conclude this section, one may wonder how robust is the infinitely degenerate ground state found for the 3-body interaction at $g = g^*$, in particular it is important to see if and how this degeneracy may be lifted by the quantum fluctuations. We point out that this highly degenerate ground state is quite peculiar, because the standard linear stability analysis of the (Hartree) mean-field solutions does not directly apply to this

case. Indeed, we remind that the results of the standard linear stability analysis of stationary spatially localized solutions of the generalized NLSE (3.1.16) can be summarized by the the Vakhitov-Kolokolov criterion [76, 77, 78]. Shortly, the criterion consists of the following: for the generalized NLSE $i\frac{\partial\psi}{\partial t} = -\frac{1}{2}\frac{\partial^2\psi}{\partial x^2} - \mathcal{F}(\mid \psi \mid)\psi$, one writes the stationary solutions in the form $\psi(x,t) = \Phi(x;\tilde{\mu})e^{-i\tilde{\mu}t}$ (where $\Phi(x;\tilde{\mu})$ vanishes for $\mid x \mid \rightarrow \infty$) and then computes the quantity $n_s(\tilde{\mu}) = \int_{-\infty}^{\infty} \mid \Phi(x;\tilde{\mu}) \mid^2 dx$. The Vakhitov-Kolokolov criterion for the onset of the soliton instability results in $dn_s(\tilde{\mu})/d\tilde{\mu} = 0$, the stability (instability) region corresponding to $dn_s(\tilde{\mu})/d\tilde{\mu} < 0$ ($dn_s(\tilde{\mu})/d\tilde{\mu} > 0$). When this criterion is applied to the PL-NLSE (3.1.13) for $\alpha = 4$, i.e. $F = -g \mid \psi \mid^4$, one obtains $\Phi(x;\tilde{\mu}) = [A/\cosh(\mathcal{K}x)]^{1/2}$, where $\tilde{\mu} = -\mathcal{K}^2/8$ and $A^2(\mathcal{K}) = 3\mathcal{K}^2/8g$. It follows $n_s(\tilde{\mu}) = \pi A(\mathcal{K})/\mathcal{K} = \sqrt{g^*/g}$, then giving $dn_s(\tilde{\mu})/d\tilde{\mu} \equiv 0$ identically for every $\tilde{\mu} < 0$. This result makes evidence of the peculiarity of the 3-body degenerate ground state and the study of its stability with respect to quantum fluctuations is therefore an interesting problem requiring an investigation going beyond the standard linear stability analysis.

3.2.1 Ground state energy

Using the bright soliton solution (3.2.29) we can now estimate the energy per particle. Going back to the physical dimensions of all quantities and normalizing now ψ_0 to $\mathcal{N}_T$, for $\alpha \neq 4$ the chemical potential is given by

$$\mu = -\frac{\hbar^2\gamma^2}{2m f_\gamma^{2\alpha/(4-\alpha)}} \left(\frac{2mG}{\hbar^2\gamma(\gamma+1)}\right)^{\frac{4}{4-\alpha}} , \tag{3.2.37}$$

where

$$f_\gamma = \frac{\sqrt{\pi}\,\Gamma(\gamma)}{\Gamma(\gamma+1/2)} .$$

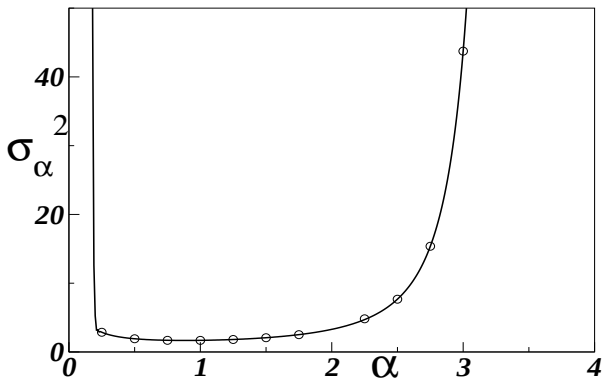

Figure 3.5: σ_α^2 versus the nonlinearity degree α. Solid line: eqn. (3.2.35); open circles: $\langle x^2 \rangle$ from the numerical determination of the ground state of the PL-NLSE (3.2.17). The value $g = 1 < g^*$ and dimensionless units are used.

The energy per particle is then obtained from the PL-NLSE energy functional

$$E_{GP} \;=\; \int dx\, \psi_0^*(x) \left[-\frac{\hbar^2}{2m} \frac{\partial^2}{\partial x^2} - \frac{2c}{\alpha+2} \mid \psi_0(x) \mid^\alpha \right] \psi_0(x) \;\; . \qquad (3.2.38)$$

Using eqn. (3.2.29) we obtain

$$\frac{E_{GP}}{\mathcal{N}_T} \;=\; -\frac{\hbar^2}{2m} \left(\frac{2mG}{\hbar^2} \right)^{\frac{4}{4-\alpha}} \mathcal{E}(\alpha) \;\; , \qquad (3.2.39)$$

where

$$\mathcal{E}(\alpha) \;=\; \left\{ \frac{1}{\gamma(\gamma+1) f_\gamma^2} \right\}^{\frac{4}{4-\alpha}} \cdot \left[\gamma^2 f_\gamma^2 - \frac{\alpha}{\alpha+2} \gamma(\gamma+1) f_\gamma f_{\gamma+1} \right] \;\; . \qquad (3.2.40)$$

For $N = 2$, $\mu = -mc^2 \mathcal{N}_T^2 / 8\hbar^2$ and the previous energy (3.1.12) is recovered. From eqn. (3.2.39) it follows that in order to maintain finite the energy per particle for large $\mathcal{N}_T$ one has to keep G fixed.

By a numerical determination of the ground state of the PL-NLSE, we have verified that (3.2.29) indeed coincides with the ground state for $\alpha < 4$

both for $g < g^*$ and $g > g^*$. In Fig. 3.6 we compare for $g = 1 < g^*$ the ground state energy per particle from eqn. (3.2.39) with the ground state energy obtained for some values of α obtained from the numerical PL-NLSE. For $g > g^*$ and $\alpha < 4$, a similar agreement is obtained.

For $\alpha = 4$, as discussed in the previous section, the chemical potential is undetermined. However, a direct substitution of (3.2.32) in (3.2.38) reveals that $E_{GP} = 0$ for $g = g^*$. Since (3.2.32) is a solution of the PL-NLSE (3.2.17) for arbitrary $\mu < 0$, and then with arbitrary width, we conclude that an infinite degeneracy - parametrized by a negative chemical potential - occurs.

Using the energy (3.2.39) we can also estimate the energy of the constant solution in the finite interval $[-L/2, L/2]$: it is $E_{const}/\mathcal{N}_T = -2c\rho^{\alpha/2}/(\alpha+2)$, where $\rho = \mathcal{N}_T/L$ is the density. To compare this energy with the previous result (3.2.39) for the bright soliton solution we have to choose how to perform the thermodynamic limit: if we choose to keep fixed the quantity $G = c\mathcal{N}_T^{\alpha/2}$, with large but finite value of $\mathcal{N}_T$, sending L to infinite the energy of the constant solution vanishes. This means that for $\alpha > 4$ the constant solution is the ground state of the system; $\alpha = 4$ and $g = g^*$ is the case in which both the solutions have zero energy.

3.3 Effect of an harmonic trap

As we have discussed in the section 1.1.1, the instability of a three-dimensional Bose gas with two-body attractive interactions can be cured by means of a harmonic trap provided if the number of particles don't exceed its critical value. In one dimension, this situation changes drastically: in fact, here a stable bright soliton there always exist.

In this section we consider the problem of analysing the effect of a harmonic trap in one dimensional Bose gas with a 3-body interaction, and more

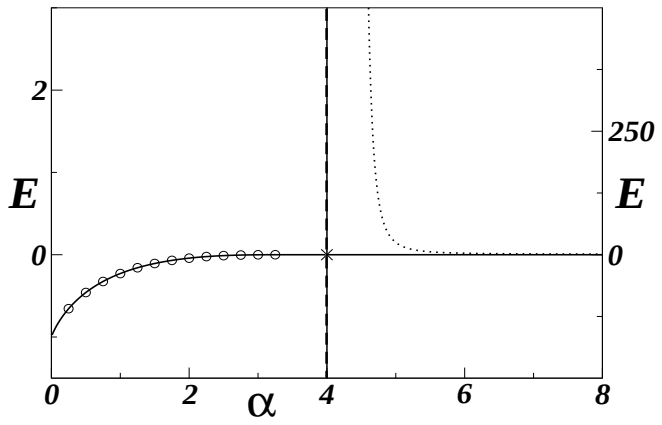

Figure 3.6: Ground state energy vs. α. Solid line (dashed line): eqn. (3.2.38) for $\alpha < 4$ ($\alpha > 4$); open circles: energy of the numerical ground state of the PL-NLSE (3.2.17). Dimensionless units (with $\mathcal{N}_T = 1$) and $g = 1 < g^*$, as well as different scales of the energy for $\alpha < 4$ (left part) and $\alpha > 4$ (right), are used.

generally, a N-body contact interaction. We show that there is a critical value c^* of the interaction, such that for $c < c^*$, the bound state is stable.

Following the procedure of section 1.1.1, we use the variational wavefunction

$$\psi_V(x) \,=\, C\, \exp(-x^2/\sigma^2) \;, \tag{3.3.41}$$

normalized to $\mathcal{N}_T$. The energy to be minimized is obtained by inserting the variational wavefunction (3.3.41) in the generalized GPE functional

$$E \,=\, \int dx \psi^*(x) \left[-\frac{\hbar^2}{2m}\frac{\partial^2}{\partial x^2} - \frac{2c}{\alpha+2} \mid \psi(x) \mid^{\alpha} + \frac{m}{2}\omega^2 x^2 \right] \psi(x) \;. \tag{3.3.42}$$

To better illustrate the peculiarities of the one-dimensional case, it is useful to perform the analysis in higher dimensions by choosing the obvious variational generalized wavefunction

$$\psi_V(x_1, \cdots, x_D) \,=\, C \exp[-\frac{(x_1^2 + \cdots + x_D^2)}{\sigma^2}], \tag{3.3.43}$$

where D is the spatial dimension.

The energy in $D = 1, 2, 3$ is then given by

$$\frac{E}{\mathcal{N}_T} = D\frac{\hbar^2}{2m\sigma^2} - cf_{\alpha,D}\frac{\mathcal{N}_T^{\frac{\alpha}{2}}}{\sigma^{\frac{D\alpha}{2}}} + D\frac{m\omega^2\sigma^2}{8} \quad , \tag{3.3.44}$$

where

$$f_{\alpha,D} \equiv \frac{2}{\alpha+2}\left(\frac{\pi}{\alpha+2}\right)^{\frac{D}{2}}\left(\frac{2}{\pi}\right)^{D\frac{\alpha+2}{4}} \quad . \tag{3.3.45}$$

Let us consider initially the homogeneous case: for $\omega = 0$ the energy (3.3.45) has a minimum only when $D\,\alpha < 4$. The critical condition is then

$$D\,\alpha = 4 \ . \tag{3.3.46}$$

For $D = 1$, the critical value corresponds to $\alpha = 4$: this is in agreement with the result of the previous section, which is now obtained by a variational approach. We observe that, without the harmonic trap, the criterion (3.3.46) can be obtained without choosing a particular variational form for the ψ, and studying the boundedness of the Hamiltonian [67]. The condition (3.3.46) is plotted in Fig.3.7, which shows that the higher N-body interactions tend to be more unstable in higher dimensions.

Let us now examine for $\omega = 0$ the critical point $D\,\alpha = 4$. The energy (3.3.44) reads

$$\frac{E}{\mathcal{N}_T f_{\alpha,D}} = \frac{1}{\sigma^2}\,(c^* - c)\,\mathcal{N}_T^{\alpha/2} \quad , \tag{3.3.47}$$

where we defined the critical value

$$c^* = \frac{D\hbar^2}{2mf_{\alpha,D}\mathcal{N}_T^{\alpha/2}} \quad : \tag{3.3.48}$$

a plot of the energy (3.3.47) is drawn in Fig.3.8. It is clear that for $c < c^*$ the energy is positive and the minimum corresponds to $\sigma \to \infty$; at variance, for $c > c^*$ the energy is negative and the minimum corresponds to $\sigma \to 0$, signaling the collapse. When $c = c^*$, the energy is zero for every width: this is how the variational approach mimics the infinite degeneracy of the ground

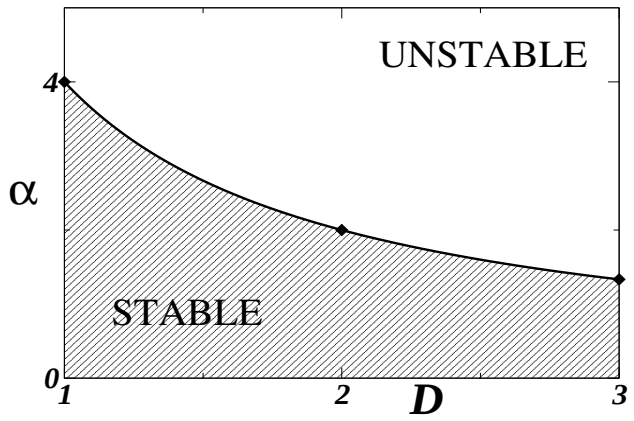

Figure 3.7: Stability region according to eqn. (3.3.46): $D = 1, 2, 3$ corresponds respectively to $\alpha = 4, 2, 4/3$, i.e. $N = 3, 2, 5/3$.

state, which was discussed in the previous section. Notice that for $D = 1$ and $\alpha = 4$ the critical value (in dimensionless units) is $g^* = 3\sqrt{3}\pi/4 \approx 4.08$, in good agreement with the analytical value $g^* = 3\pi^2/8 \approx 3.70$.

When the harmonic trap is present ($\omega \neq 0$), there is still a minimum when $\alpha < 4/D$. When $D\alpha > 4$, we can identify the critical value c^* as indicated in [32] for the $D = 3$ and $\alpha = 2$ case: since $E \to -\infty$ for $\sigma \to 0$ and $E \to \infty$ for $\sigma \to \infty$, the critical value is obtained by the conditions $\partial E/\partial\sigma = \partial^2 E/\partial\sigma^2 = 0$. In this way we arrive to the result

$$c^* \mathcal{N}_T^{\frac{\alpha}{2}} = \left(\frac{D\alpha - 4}{4m\omega^2}\right)^{\frac{D\alpha-4}{8}} \left(\frac{16\hbar^2}{m(D\alpha+4)}\right)^{\frac{D\alpha+4}{8}} \frac{\alpha+2}{2\alpha} \left(\frac{\alpha+2}{\pi}\right)^{\frac{D}{2}} \left(\frac{\pi}{2}\right)^{D\frac{\alpha+2}{4}} . \tag{3.3.49}$$

For $c < c^*$ there is a minimum and the system is stable, while for c^* the energy does not have ever a minimum: hence, irrespectively of how large ω may be, the system always collapses. For $\omega = 0$ (no trap) and $c < c^*$ ($c > c^*$), the minimum value of the energy is then obtained for $\sigma = 0$ ($\sigma = \infty$).

The instability curve (3.3.49) depends on D: with dimensionless units

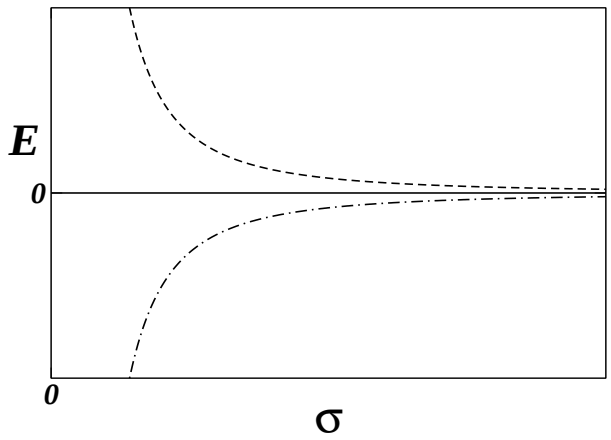

Figure 3.8: Plot of the variational energy (3.3.44) vs. σ at the critical point $D\alpha = 4$ for $\omega = 0$: the dashed, dot-dashed and solid lines correspond respectively to $c < c^*$, $c > c^*$ and $c = 0$, with c^* given by eqn. (3.3.48).

(and $\mathcal{N}_T = 1$), in one dimension as $\alpha \to \infty$ the critical value g^* goes to zero for $\omega \geq \pi$ and to infinity otherwise; in two dimensions the behaviour is similar except that $g^* \to \pi/e$ when $\omega = \pi$; while in three dimensions critical value goes to infinity for $\pi \geq \omega$ and to zero otherwise. A plot of g^* in $D = 1$ for $\alpha > 4$ is presented in Fig. 3.9.

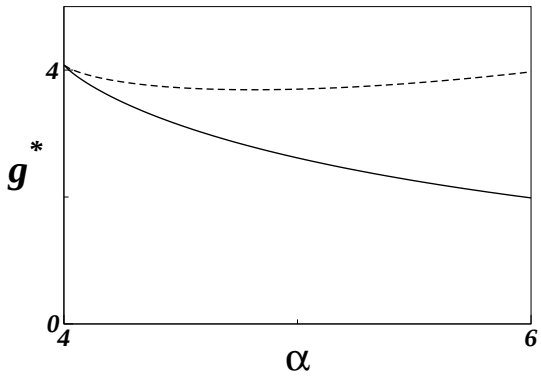

Figure 3.9: Critical value g^* vs. α for $\alpha > 4$, with $D = 1$. Dimensionless units (with $g = \mathcal{N}_T = 1$) are used, with $\omega = 1$ (dashed line) and $\omega = 4$ (solid line).

Chapter 4

Ultracold Bosons with 3-Body Attractive Interactions in an Optical Lattice

The mean-field dynamics for BECs loaded into the OL is described by the cubic Gross-Pitaevskii equation (GPE) with a periodic potential [2, 3, 79]. The respective Bogoliubov's excitation spectrum features a band structure, similar to the electronic Bloch bands in solid state. If the OL potential is deep enough, the lowest-band dynamics maps into a discrete nonlinear Schrödinger (NLS) equation [80]. Using this correspondence, the BEC dynamics was studied in the framework of the nonlinear-lattice theory [80, 81, 82, 83]. The presence of the OL gives raise to the occurrence of energetic and dynamical instabilities, which have been predicted theoretically [84, 85, 86, 87, 88, 89, 90, 91] and studied experimentally [92, 93].

Another important application of the OLs is their use in the manipulation and control of the dynamics of matter-wave solitons: the periodic potential allows for the creation of localized gap solitons even in case of the repulsive two-body interaction, as it has been shown in the experiment [94]

(with the attractive interactions, bright matter-wave solitons were created and observed in condensates of ^{7}Li [35, 37] and ^{85}Rb [**?**] atoms). More generally, the possibility to use space- and time- dependent modulating fields acting on atoms is a powerful way to control soliton properties [29]: for instance, while the GPE without external potentials admits stable soliton solutions only in the 1D geometry [28, 25], periodic potentials can stabilize soliton solutions even in higher dimensions [95, 96].

As we have seen in the previous chapter, in presence of three-body interactions ($N = 3$), the system is described by a *quintic* GPE, i.e. the respective nonlinear term in the energy density is proportional to $|\psi|^6$, where ψ is the single-atom mean-field wave function (a similar term accounting for the two-body interactions, $N = 2$, is proportional to $|\psi|^4$).

For $N = 3$, normalizable soliton solutions exist only at a critical value of the interaction strength, at which an infinite degeneracy of the ground states occurs [31]: wave functions $\psi(x) = \text{const} \cdot \cosh^{-1/2}(x/\sigma)$ with arbitrary width σ are solutions to the time-independent quintic GPE having the same energy, but different values of the chemical potential. A relevant issue is how this infinite degeneracy is lifted by a periodic potential like the one created by an OL [95, 97].

When the two-body interaction is present, the mean-field equation is a cubic-quintic (CQ) GPE [97, 98]. In particular, if the two-body interaction is repulsive while its three-body counterpart is attractive, soliton solutions to the CQ GPE can be found in an exact analytical form (in the absence of an external potential), but they are unstable [98], see section 4.1.1 below. The issue we address in this chapter is the possibility to stabilize such localized solitons by adding an OL. Recently it has been shown [19] that it is possible to tune the two-body interaction independently from the three-body ones. It is relevant to mention that, in the framework of the effective GPE for the BEC loaded into a nearly 1D ("cigar-shaped") trap, with tight

transverse confinement, an effective *attractive* quintic term appears in the absence of any three-atom interactions, as a manifestation of the deviation from the one-dimensionality [99, 98]. We also mention that in pure one-dimensional case the CQ GPE equation arises only if the three-body losses are negligible.

Apart from the BEC context, where the nonlinearity degree is related to the number of atoms simultaneously involved in the microscopic contact interaction, the quintic NLS equation and, more generally, ones with the power-law and CQ nonlinearities are also important as models of the light propagation in self-focusing media [100]. In the cubic case (Kerr medium), the effect of imprinted optical lattices have been investigated both in local [101, 95] and non-local [102, 103] models. In Refs. [95, 101, 96, 104, 105] it was shown that the addition of an OL stabilizes solitons against the collapse in every dimension, the peculiarity of one-dimensional cubic GPE being the absence of a threshold (minimum necessary norm) for the existence of the soliton.

In this chapter, we study effects of the OL on the existence and stability of localized states of the 1D boson gas with three-body contact interactions. First, we look for soliton solutions to the quintic GPE in the presence of the periodic potential by introducing a variational wave function (*ansatz*), which is modeled on the respective Townes-type soliton, i.e., it yields the exact solution in the absence of the lattice, and analyze energy minima corresponding to this ansatz. The OL with any value of its strength (i.e., with zero threshold) opens a stability window around the critical point [97], where the soliton solutions are stable, as we discuss in Section II.

A new situation arises when the repulsive cubic (two-body) interaction is added to the quintic (three-body) attractive term. In the absence of the external potential, the respective solitons are *strongly unstable*, in the sense of having an unstable eigenvalue in the Bogoliubov - de Gennes spectrum

of small perturbations around them [98], while the Townes solitons in the quintic equation are, in the same sense, neutrally stable degenerate objects, whose actual instability is subexponential, being accounted for by a zero eigenvalue. We demonstrate that the OL opens a stability window for solitons in this situation too, but only if the lattice strength exceeds a *finite* threshold value.

The plan of the chapter is as follows. In the section 4.1 the properties of the (unstable) soliton solutions to power-law GPE equation are summarized and cubic-quintic (CQ) GPE corresponding to the mean-field description of the 1D Bose gas with two-body repulsive and three-body attractive interactions is introduced. In the sections 4.2 and 4.3, we use the variational approximation (VA)[109] to discuss the effect of the OL on solitons. We introduce an appropriate ansatz and compute the corresponding energy. The limit of the vanishing two-body interaction is considered and compared with previous results [97]. In section 4.4, the stability region for the soliton solution in the presence of the repulsive two-body interaction and OL is determined and compared with numerical findings. The effect of an additional harmonic-trap potential is studied in section 4.5, wher it will be shown that the stability region depends on the matching between minima of the periodic potential and the location of the minimum of the harmonic trap.

4.1 The model

The quantum many-body Hamiltonian for the 1D Bose gas with N-body contact attractive interactions loaded in an external potential is

$$\hat{H}=\int_{-\infty}^{+\infty}dx\left\{\hat{\Psi}^{\dagger}(x)\hat{T}\hat{\Psi}(x)-\frac{c}{N!}\left[\hat{\Psi}^{\dagger}(x)\right]^{N}\left[\hat{\Psi}(x)\right]^{\mathcal{N}}+\hat{\Psi}^{\dagger}(x)V_{ext}(x)\hat{\Psi}(x)\right\}, \tag{4.1.1}$$

where $\hat{T} = -(\hbar^2/2m)\,\partial^2/\partial x^2$ is the kinetic-energy operator, $\hat{\Psi}(x)$ the bosonic-field operator, $c > 0$ the interaction strength and $V_{ext}(x)$ the external potential.

In the mean-field approximation, the classical counterpart of quantum Hamiltonian (4.1.1) is

$$E = \int dx\, \psi^*(x) \left[\hat{T} - \frac{2c}{\alpha+2}|\psi(x)|^\alpha + V_{ext}(x)\right] \psi(x), \tag{4.1.2}$$

and the respective 1D dynamics obeys the power-law GPE:

$$i\hbar\frac{\partial\psi(x,t)}{\partial t} = \left(-\frac{\hbar^2}{2m}\frac{\partial^2}{\partial x^2} - c|\psi(x,t)|^\alpha + V_{ext}(x)\right)\psi(x,t), \tag{4.1.3}$$

where macroscopic wave function $\psi(x,t)$ is normalized to the total number of atoms, $\mathcal{N}_T$, and the nonlinearity degree is related to the order of the multi-body interactions N by

$$\alpha = 2\,(N-1)\ . \tag{4.1.4}$$

In eqn. (4.1.3), $V_{ext}(x)$ typically includes a superposition of an harmonic trap and periodic potential

$$V_{\rm ext}(x) = V_H(x) + V_{OL}(x) \tag{4.1.5}$$

so that $V_H(x) = m\,\omega^2 x^2/2$ and $V_{OL} = \epsilon\,\sin^2(qx+\delta)$, where ϵ is proportional to the power of the laser beams which build the OL, and $q = 2\pi/\lambda$, with $\lambda = \lambda_{\rm laser}\sin(\theta/2)$, $\lambda_{\rm laser}$ being the wavelength of the beams, and θ the angle between them (the period of the lattice is $\lambda/2$). Parameter δ corresponds to a mismatch between minima of the lattice potential V_{OL} and the minimum (at $x = 0$) of the parabolic potential V_H: when $\delta = 0$ ($\delta = \pi/2$) a minimum (maximum) of V_{OL} coincides with the minimum of V_H. Except for the last section , we consider the situation without the parabolic trap (i.e., $\omega = 0$), therefore we set $\delta = 0$.

The time-independent power-law GPE corresponding to eqn. (4.1.3) is

$$\left[-\frac{1}{2}\frac{d^2}{dx^2} - c|\psi(x)|^\alpha + V_{\rm ext}(x)\right]\psi(x) \;=\; \mu\psi(x), \tag{4.1.6}$$

where μ is the chemical potential, $V_{ext}(x) \equiv \epsilon \sin^2(qx)$, and the wave function is normalized to 1. Let us keep in mind that, if one fixes coefficient c in front of the interaction term, the Townes solitons exist for a particular value of the norm of the wave function [106, 97]. On the other hand, fixing the normalization of the wave function (in our units, the norm is 1) amounts, for $\alpha \neq 4$, to fixing a relation among the chemical potential and the interaction strength [31], so that for each c it is possible to obtain a single soliton solution (although, in the infinite system, these solutions provide the ground state only for $\alpha < 4$, i.e. for $N < 3$).

As we have seen in the previous chapter, for the attractive three-body interactions, eqn. (4.1.6) reduces to

$$\left[-\frac{1}{2}\frac{\partial^2}{\partial x^2} - c|\psi(x)|^4 + V_{\rm ext}(x)\right]\psi(x) \;=\; \mu\psi(x). \tag{4.1.7}$$

where the chemical potential μremains indefinite, assuming arbitrary negative values, while the soliton solution of the form

$$\psi(x) \;=\; \frac{(3k^2/8c)^{1/4}}{\sqrt{\cosh(kx)}}\,,\; k^2 = -8\mu \tag{4.1.8}$$

satisfies the unitary normalization condition at a single (critical) value of the interaction strength [106, 31],

$$c = c^* \;\equiv\; 3\pi^2/8. \tag{4.1.9}$$

At $c = c^*$, all solutions (4.1.8) share a common value of the energy, which is simply $E = 0$ [97, 31], as follows from Eqs. (3.3.42) and (4.1.9).

When, besides the three-body attractive interaction, the two-body interaction is present, the mean-field equation is the GPE with the CQ nonlinearity,

$$\left[-\frac{1}{2}\frac{d^2}{dx^2} + g|\psi(x)|^2 - c|\psi(x)|^4 + V_{\rm ext}(x)\right]\psi(x) \;=\; \mu\psi(x)\,. \tag{4.1.10}$$

As said above, we chiefly focus on the case of the *repulsive* two-body interaction, i.e. $g \geq 0$. As we will show in the next section, a family of exact soliton solutions to Eq, (4.1.10) for $V_{ext}(x) = 0$ can be obtained in the exact form [107, 108, 98], which is, for $g \geq 0$, the following

$$\psi^2(x) \;=\; \frac{A^2}{(1+\xi A^2)\cosh\left(2\sqrt{2|\mu|}x\right) - \xi A^2}, \tag{4.1.11}$$

where $\xi = g/\left(4|\mu|\right)$, and A^2 is the maximum value of the density, at the soliton center, which is expressed in terms of other parameters,

$$A^2 = \frac{3}{c}\left(\frac{g}{4} + \sqrt{\frac{g^2}{16} + \frac{c|\mu|}{3}}\right). \tag{4.1.12}$$

Obviously, for $g = 0$ solution (4.1.11) reduces to the Townes soliton (4.1.8).

Imposing the above-mentioned normalization,

$$\int_{-\infty}^{+\infty} |\psi(x)|^2 dx = 1, \tag{4.1.13}$$

on solution (4.1.11), one arrives at relation

$$\sqrt{\frac{6}{c}}\tan^{-1}\left(\sqrt{1+2\xi A^2}\right) \;= 1\,, \tag{4.1.14}$$

from where it follows that, for $g > 0$, solutions with a negative chemical potential satisfying the normalization condition exists for $c > c^*$.

4.1.1 Localized solutions of the cubic-quintic Gross-Pitaevskii equation

Assuming that $\psi(x)$ is real, we look for localized solutions to the CQ NLS equation,

$$-\frac{1}{2}\frac{d^2\psi}{dx^2} + g\psi^3 - c\psi^5 \;=\; \mu\psi \tag{4.1.15}$$

with $c > 0$ and $g \geq 0$. Interpreting x as a formal time variable and $\psi(x)$ as the coordinate of a particle, eqn. (4.1.15) formally corresponds to the Newton's equation of motion of this particle,

$$M\frac{d^2\psi}{dx^2} \;=\; -\frac{\partial V}{\partial \psi}\,, \tag{4.1.16}$$

where the effective mass is $M = 1/2$, and the potential is

$$V(\psi) \,=\, \frac{\mu}{2}\psi^2 - \frac{g}{4}\psi^4 + \frac{c}{6}\psi^6 \;, \tag{4.1.17}$$

where an arbitrary additive constant was chosen so as to have $V(0) = 0$. Potential (4.1.17) for $\mu < 0$, which corresponds to normalizable solutions, is plotted in Fig. (3.2.21). Condition $V(\pm A) = 0$ yields expression (4.1.12) for the soliton amplitude.

Making use of the conservation of the corresponding Hamiltonian,

$$H = \frac{M}{2}\left(\frac{d\psi}{dx}\right)^2 + V(\psi), \tag{4.1.18}$$

and the boundary conditions for localized solutions: $\psi(x \to \infty) \to 0$, $d\psi/dx(x \to \infty) \to 0$, one has $H = 0$. Taking into regard the fact that $V(\psi) \leq 0$ for $0 \leq \psi \leq A$, and looking for solutions with $d\psi/dx < 0$ at $x > 0$, one obtains

$$x \,=\, \int_{\psi(x)}^{A} \frac{d\psi}{2\sqrt{-V(\psi)}}, \tag{4.1.19}$$

from where it follows

$$\mathcal{E} \,=\, \frac{\psi^2(x)}{A^2}\frac{2a^2 + b^2A^2}{2a^2 + b^2\psi^2(x) + 2a\sqrt{a^2 + b^2\psi^2(x) - \psi^4(x)}}, \tag{4.1.20}$$

with $\mathcal{E} \equiv e^{-2\sqrt{2|\mu|}x}$. In eqn. (4.1.20), we use notation $a^2 = 3|\mu|/c$ and $b^2 = 3g/2c$. Thus, from eqn. (4.1.20) one obtains

$$\psi^2(x) \,=\, \frac{4a^2A^2\left(2a^2 + b^2A^2\right)\mathcal{E}}{\left[2a^2 + b^2A^2\left(1 - \mathcal{E}\right)\right]^2 + 4a^2A^4\mathcal{E}^2}\,. \tag{4.1.21}$$

One can easily check that this expression yields $\psi^2(x) = A^2/\cosh\left(2\sqrt{2|\mu|}x\right)$ for $g = 0$, and that $\psi(0) = A$, as it must be. Finally, using relation $a^2 + b^2A^2 = A^4$, one obtains eqn. (4.1.11) from eqn. (4.1.21), after some algebra.

However, such localized solutions are unstable [98] (in particular, because they do not satisfy the Vakhitov-Kolokolov stability criterion [76]). In the following section we will discuss how the OL can stabilize such localized solutions.

4.2 Variational approximation

Both for $\alpha = 2$ and 4 ($\mathcal{N} = 2$ and 3), and for the GPE with the mixed CQ nonlinearity, the presence of the periodic potential makes it necessary to resort to approximate methods for finding solitons. To this end, we resort to the VA (variational approximation) [57, 109] based on the *ansatz* which yields exact soliton solution (4.1.8) of the quintic NLS equation in the absence of the external potential:

$$\psi_V(x) = \frac{A}{\sqrt{\cosh(x/\sigma)}} \, . \tag{4.2.22}$$

Here, width σ is the variational parameter to be determined by the minimization of the energy, while amplitude A will be found from normalization condition (4.1.13). We expect that ansatz (4.2.22), which does not explicitly include the modulation of the wave function induced by the OL, may give a reasonable estimate of the soliton energy for small values of ϵ, cf. the known result for the 2D equation with the cubic nonlinearity ($\alpha = 2$) and OL potential [95, 104]. In the case of the 3D GPE which includes the cubic term and harmonic trap, this approach leads to an estimate for the critical value of the number of atoms above which the condensate collapses, which was shown to be in a reasonable agreement with results produced by the numerical solution of the GPE [32, 33]. In one dimension, the VA based on the simple Gaussian ansatz leads to a conclusion that the wave function of the ground state is localized even in the absence of the harmonic trap [110], in agreement with the obvious fact that the single-soliton solution represents the ground state in that case. Similar analyses carried out in the model including the cubic term and OL [101, 95, 111] have demonstrated that, unlike the 2D and 3D cases, in one dimension the soliton does not have an existence threshold in terms of its norm (number of atoms).

The energy to be minimized is obtained by inserting ansatz (4.2.22) in the GPE energy functional given by eqn. (3.3.42). The kinetic and quintic-

interaction energy terms in the functional both scale as σ^{-2}; then, the energy per particle computed from expression (3.3.42) is

$$E = \frac{\beta}{\sigma^2} + \frac{g}{\pi^2\sigma} + \frac{\epsilon}{2}\left[1 - \mathrm{sech}(\pi q\sigma)\right], \tag{4.2.23}$$

$$\beta \equiv \frac{1}{16} - \frac{c}{6\pi^2} = \frac{c^* - c}{6\pi^2}, \tag{4.2.24}$$

where c^* is defined in eqn. (4.1.9).

For $\epsilon = 0$ (without the OL), the scenario discussed in the previous section for the uniform CQ GPE with the attractive three-body and repulsive two-body interactions is recovered, as energy (4.2.23) reduces in that case to

$$E = \frac{\beta}{\sigma^2} + \frac{g}{\pi^2\sigma}. \tag{4.2.25}$$

For $g = 0$, the energy is positive when $c < c^*$ (i.e., $\beta > 0$) and vanishes at $\sigma \to \infty$; for $c = c^*$ (i.e., $\beta = 0$) one obtains $E = 0$, in agreement with the above-mentioned exact result showing the infinite degeneracy of soliton family (4.1.8), while for $c > c^*$ the energy is negative and diverges (to $-\infty$) for $\sigma \to 0$, signaling, in terms of the VA, the onset of the collapse. With $g > 0$, expression (4.2.25) does not give rise any minimum of the energy, which agrees with the known fact of the absence of stable solitons in this case [98].

A detailed study of minima of variational energy (4.2.23) is presented in 4.6. In the following subsection, we consider the case of the self-focusing quintic GPE in the presence of the OL ($\epsilon > 0,\ g = 0$), while the discussion of the general case ($g > 0$) is given in section 4.4.

4.3 Self-focusing quintic GPE with the optical-lattice potential

Here we address the stability of localized variational mode (4.2.22), for different values the OL parameters, strength ϵ and wavenumber q, keeping

$g = 0$. The results of the analysis of minima of the variational energy (4.2.23), presented in section 4.6, can be summarized as follows (see also Fig. 4.1): for $c \geq c^*$, the infinitely deep minimum of the energy is obtained for $\sigma \to 0$, which corresponds to the collapse, as shown in Fig. 4.1(a). For $c < c^*$, the collapse may be avoided, and three possibilities arise: there exists another special value $c' < c^*$, such that for every c between c' and c^* the energy has a minimum at $\sigma = \sigma_1$ and a maximum at $\sigma = \sigma_2$, while for $c < c'$ the energy does not have a minimum at any finite value of σ, see Fig. 4.1(d). Further, two different situations should be distinguished for c between c' and c^*: there exists a specific value (see 4.6)

$$c^{**} = c^* - \frac{3\epsilon}{2q^2} T_c \,, \text{ where } T_c \approx 2.13, \tag{4.3.26}$$

(with $c^{**} > c'$) such that, for $c^{**} < c < c^*$, the energy has a *global* minimum at $\sigma = \sigma_1$ (which, thus, represents the *ground state* of the boson gas in this situation), while, for $c' < c < c^{**}$, the energy minimum at $\sigma = \sigma_1$ is a *local* one. In other words, since the energy tends to value $\epsilon/2$ at large σ, for $c^{**} < c < c^*$ ($c' < c < c^{**}$) it satisfies inequality $E(\sigma_1) < \epsilon/2$ ($E(\sigma_1) > \epsilon/2$), as showed in Figs. 4.1(b,c).

From the above analysis, we infer the VA predicts that, for $c < c^{**}$, the ground state is a delocalized one, for $c > c^*$ it is collapsing, and for $c^{**} < c < c^*$ it is represented by a finite-size soliton configuration (in agreement with Ref. [97]). Equation (4.3.26) shows that the width of the stability region depends on ratio ϵ/q^2: keeping fixed all other parameters, the decrease of the lattice spacing (i.e., the increase of q) leads to a reduction of the stability region. Equation (4.3.26) also shows that for $\epsilon/q^2 = 2c^*/3T_c \approx 1.16$ one has $c^{**} = 0$: however, for $c = 0$, the ground state is delocalized, hence variational ansatz (4.2.22) becomes irrelevant, as it does not take into account the modulation induced by the deep OL potential.

In Fig. (4.2), we plot a numerically found ground state of the quintic

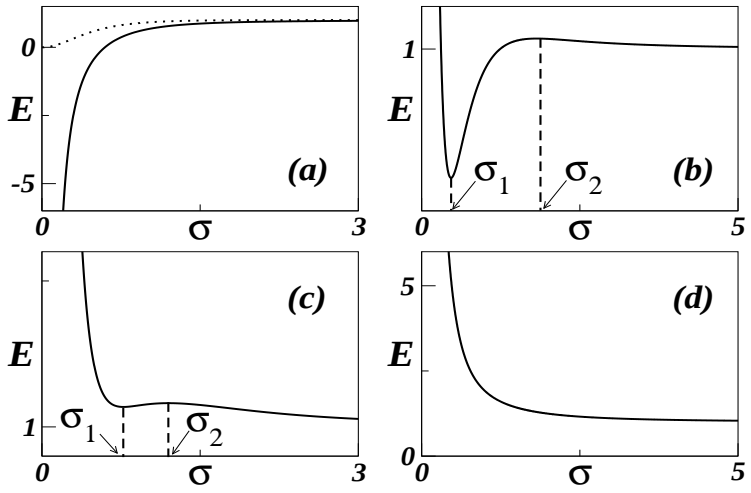

Figure 4.1: Variational energy E versus σ (in units of $\epsilon/2$) for $c \geq c^*$ (a); $c^{**} < c < c^*$ (b); $c' < c < c^{**}$ (c); $c < c'$ (d). In (a) the dotted (solid) line is the energy for $c > c^*$ ($c = c^*$); in (b)-(c), points of the energy minimum and maximum, σ_1 and σ_2, are indicated.

GPE in a 1D box (x is taken between $-L$ and L, with $L = 10$). It is seen that, with the increase of $c^* - c$, the configuration becomes broader and broader, until a critical value is reached, as discussed in [97]. In the inset of Fig. (4.2) we plot the width of the numerically found ground state versus c, which makes the delocalization transition evident. Variational estimate (4.3.26) for the critical value of $c^* - c$, as predicted by the variational approximation [see eqn. (4.3.26)], is displayed in Fig. (4.3) together with numerical results. One observes sees a reasonable agreement between them, especially for small ϵ, which is due both to the use of the more adequate ansatz (4.2.22), rather than a Gaussian, and also because T_c is found as the value at which the global (rather than local) minimum disappears.

4.4 The stability region for the condensate with the competing two- and three-body interactions

The most interesting situation is that when the two-body repulsive interaction (with $g > 0$) competes with the the attractive three-body collisions ($c > 0$). As mentioned above, all solitons in the free space ($\epsilon = 0$) are strongly unstable in this situation [98], and the possibility of their stabilization by the OL was not studied before. The analysis of variational energy (4.2.23), presented in 4.6, yields the following results for this case. For $c > c^*$, the energy does not have a minimum at finite σ, hence the OL cannot stabilize the solitons. If $c = c^*$, the energy has a global minimum at finite value of σ when

$$G \equiv \frac{2gq}{\pi\epsilon} < G_c \approx 0.663 \; . \tag{4.4.27}$$

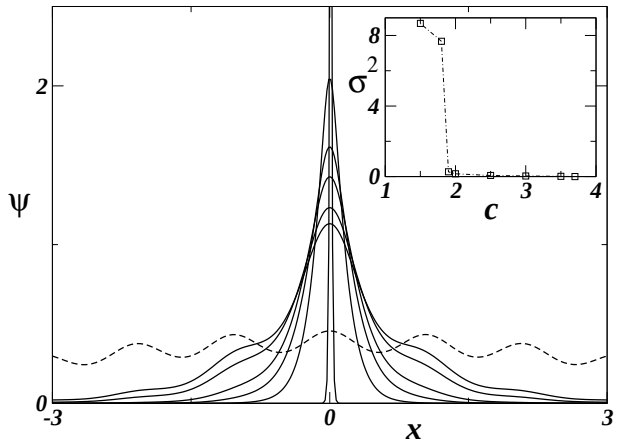

Figure 4.2: The numerically found ground state of the quintic GPE with the periodic (OL) potential, for several values of nonlinearity coefficient c. Solid lines, starting from the narrowest configuration, refer to $c = 3.7, 3.5, 3, 2.5, 2, 1.9$ (recall that $c^* = 3\pi^2/8 \simeq 3.701$), and the dashed line – to $c = 1.8$. Inset: width σ of the ground state as a function of c (the dot-dashed line is a guide to the eye). Critical value c^{**} obtained from the numerical analysis is $c^{**} = 1.87(3)$, which should be compared with value (4.3.26) predicted by the variational approximation, $c^{**} \simeq 1.57$. parameters of the OL are $\epsilon = 6$ and $q = 3$.

For $c < c^*$, the energy features a global minimum at finite σ for $c^{**}(G) < c < c^*$, where the critical value is given by

$$c^{**}(G) \equiv c^* - \frac{3\epsilon}{2q^2} T_c(G)\,, \tag{4.4.28}$$

cf. definition (4.3.26) for $G = 0$. The value T_c depends upon G, vanishing for G larger than some critical value, $G_{\rm crit}$. This means that, to balance the destabilizing effect of the repulsive two-body interactions, the strength of the periodic potential, ϵ, must *exceed* its own critical value,

$$\epsilon_{\rm crit} = \frac{2qg}{\pi G_{\rm crit}}\,. \tag{4.4.29}$$

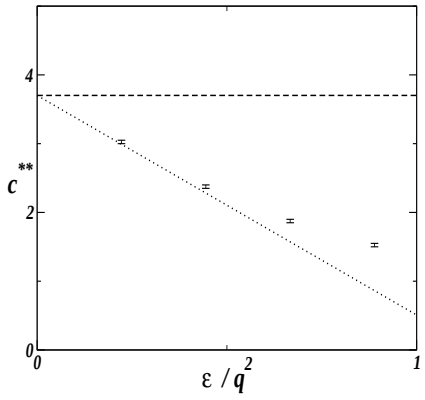

Figure 4.3: Dotted line: the variational estimate for c^{**} as a function of ϵ/q^2, according eqn. (4.3.26), the dashed line corresponding to $c^* = 3\pi^2/8$. Discrete symbols represent results obtained from the numerical solution of the quintic GPE. They designate the transition form the localized ground state to the extended one (parameters are the same as in Fig. (4.2). According to the variational approximation, the ground state is delocalized ($\sigma \to \infty$) below the dotted line, and it collapses ($\sigma \to 0$) for c above the dashed line.

Otherwise, eqn. (4.4.28) yields $c^{**} = c^*$, and the OL cannot stabilize the solitons.

In Fig. (4.4) we plot the numerically found ground-state of CQ GPE (4.1.10) as a function of ϵ, for a particular choice of parameters. It is seen that, at small ϵ, the wave function ψ remains delocalized, until a critical value is reached. In the inset of Fig. (4.4) the width of the numerically generated ground state is plotted versus ϵ. The comparison between variational estimate (4.4.29) and numerical results is reasonable, and it can be further improved by choosing a variational wave function which, in the limit of $\epsilon = 0$ (uniform space) reproduces exact CQ soliton (4.1.11). In Fig. (4.5), we compare critical value $\epsilon_{\rm crit}$, as given by eqn. (4.4.29), with

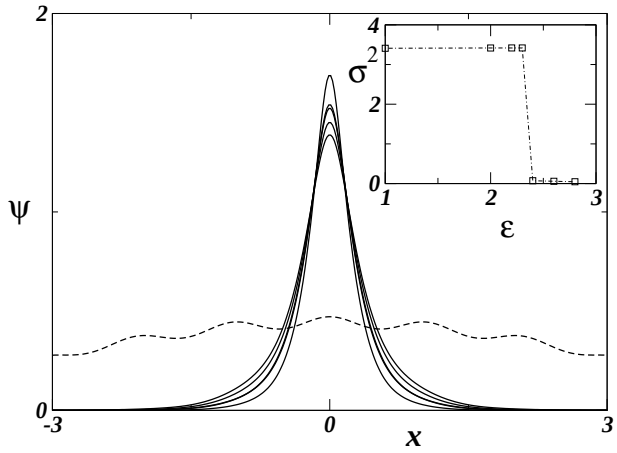

Figure 4.4: The numerically found ground state of the cubic-quintic GPE for several values of ϵ. Solid lines, starting from the narrowest wave function, refer to $\epsilon = 4, 3, 2.8, 2.6, 2.4$, and the dashed line – to $\epsilon = 2.3$. Inset: the width of the ground state versus ϵ (the dot-dashed line is a guide to the eye). Critical value $\epsilon_{\rm crit}$ obtained from the numerical data is $\epsilon_{\rm crit} = 2.35(5)$, which should be compared to the value given by eqn.(4.4.29), which is $\epsilon_{\rm crit} \simeq 2.88$. The parameters are $c = 3.65$, $g = 1$, $q = 3$, $L = 5$.

numerical results: for small g, the predicted linear dependence of $\epsilon_{\rm crit}$ on g is well corroborated by the numerical results, the relative error in the slope being $\sim 20\%$.

4.5 The effect of the harmonic trap

In this section we use the variational approximation based on ansatz (3.3.41) to examine the combined effect of the parabolic trapping potential acting together with an OL, i.e., we take the external potential as

$$V_{\rm ext}(x) \, = \, \omega^2 x^2/2 + \epsilon \, \sin^2 \left(qx + \delta \right) \ , \qquad (4.5.30)$$

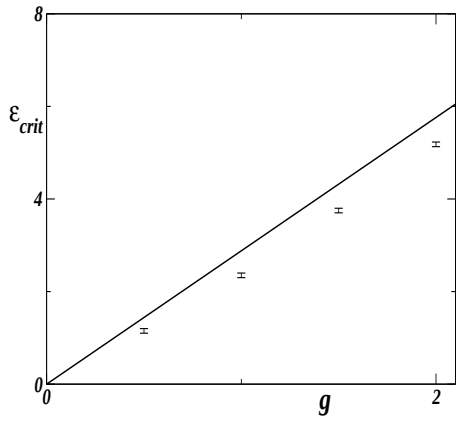

Figure 4.5: Solid line: ϵ_{crit} vs. g given by eqn. (4.4.29). Symbols refer to results obtained from the numerical solution for the ground state of the cubic-quintic GPE. They represent the delocalization transition. The parameters as the same in Fig. (4.4).

focusing on the limit of $g = 0$ (no binary collisions). Value $\delta = 0$ ($\delta = \pi$) corresponds to the match (mismatch) between the minimum of the harmonic potential and a local minima of the lattice potential. The respective variational energy is obtained from (4.1.2) with potential (4.5.30), and it is given by

$$E = \frac{\beta}{\sigma^2} + \frac{\pi^2\omega^2\sigma^2}{8} + \frac{\epsilon}{2}\left[1 - \cos(2\delta)\text{sech}(\pi q\sigma)\right]. \tag{4.5.31}$$

With $\cos(2\delta) \geq 0$, the system is stable for $c < c^*$, and it collapses otherwise. With $\cos(2\delta) < 0$, a richer behavior is predicted by the VA. The system does stabilize for $c < c^*$, while, for $c > c^*$, the presence of the mismatched harmonic trap gives rise to a metastability region. Since $E \to -\infty$ as $\sigma \to 0$ and $E \to +\infty$ as $\sigma \to \infty$, one can encounter two possibilities: either $\partial E/\partial\sigma$ is positive for all σ (and there are no energy minima), or equation $\partial E/\partial\sigma = 0$ has two roots, corresponding to a local minimum and a maximum. The equation for the value of σ at which energy

(4.5.31) reaches a local minimum is

$$|\beta| \;=\; \frac{\epsilon\,|\cos(2\delta)|}{4\pi^2 q^2}\ell(\theta), \tag{4.5.32}$$

where $\theta \equiv \pi q\sigma$, and

$$\ell(\theta) \equiv \theta^3\left(\frac{\sinh\theta}{\cosh^2\theta} - \eta\theta\right), \tag{4.5.33}$$

$$\eta \;\equiv\; \frac{\omega^2}{2\epsilon q^2 \mid cos(2\delta)\mid}. \tag{4.5.34}$$

One sees that, for $c = c^*$ (i.e., $\beta = 0$), eqn. (4.5.32) does not have a nonvanishing solution if q is smaller than a critical value,

$$q^{(\mathrm{cr})} \;=\; \frac{\omega}{\sqrt{2\epsilon\,|\cos(2\delta)|}}, \tag{4.5.35}$$

while it has a nonvanishing solution for $q > q^{(\mathrm{cr})}$.

Actually, for $c > c^*$ (i.e., $\beta < 0$), eqn. (4.5.32) with $q > q^{(\mathrm{cr})}$ has two nonvanishing roots, one of which is a local minimum, while such roots do not exist for $q < q^{(\mathrm{cr})}$. For $q > q^{(\mathrm{cr})}$, the right-hand side. of eqn. (4.5.32) has a maximum value, which fixes the maximum value of β, i.e. the maximum value of c, to which we refer as c^{***}. Then, for $c > c^{***}$, the variational energy does not have a local minimum. For $c^* < c < c^{***}$ there appears a finite metastability region, in terms of wavenumber q, as illustrated by Fig. 4.6. In other words, for c fixed, metastable states appear at large values of ϵ.

4.6 The variational energy

In this section we aim to study minima of variational energy (4.2.23). When $g = 0$, one sees that, for $c > c^*$, the energy per particle tends to $-\infty$ at $\sigma \to 0$, and $\epsilon/2$ at $\sigma \to \infty$. Then, with regard to $\partial E/\partial\sigma > 0$, no local (metastable) minima exist, and variational wave function (4.2.22) is not

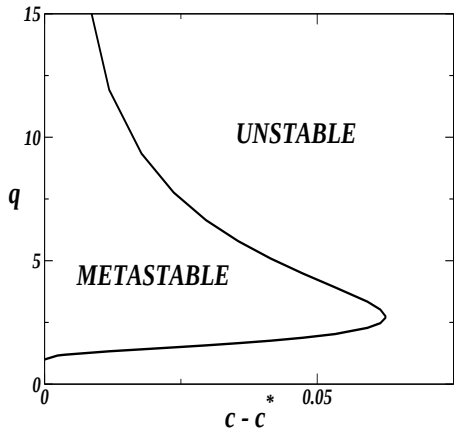

Figure 4.6: The critical line separating in the $(q, c - c^*)$ plane of the model (including the parabolic trap) the metastable region from the unstable one. Values $\epsilon = 1$, $\cos(2\delta) = -0.5$, and $\omega = 1$ were chosen here.

the ground state for any finite width. For $c = c^*$, one obtains the global minimum at $\sigma = 0$, which implies the collapse. For $c < c^*$, the situation is different: $E \to \infty$ as $\sigma \to 0$ (because $\beta > 0$), and $E - \epsilon/2 \to +0$ as $\sigma \to \infty$. Then one has to find out for what value of β derivative $\partial E/\partial\sigma$ has two real zeros. Introducing parameter

$$T = \frac{4\beta\pi^2 q^2}{\epsilon}, \tag{4.6.36}$$

with β defined as per eqn. (4.2.24), one can write condition $\partial E/\partial\sigma = 0$ as

$$T = \theta^3 \frac{\sinh\theta}{\cosh^2\theta}, \tag{4.6.37}$$

where $\theta = \pi q\sigma$, as defined above. Equation (4.6.37) can be satisfied if T is smaller than a maximum value $T' \approx 2.67$, and it then has two roots, θ_1 and θ_2, which correspond, respectively to the minimum at $\sigma = \sigma_1$, and maximum at $\sigma = \sigma_2$ (see Fig. (4.1)). For $T > T'$, eqn. (4.6.36) has no roots, hence the variational energy has no minima at finite values of the

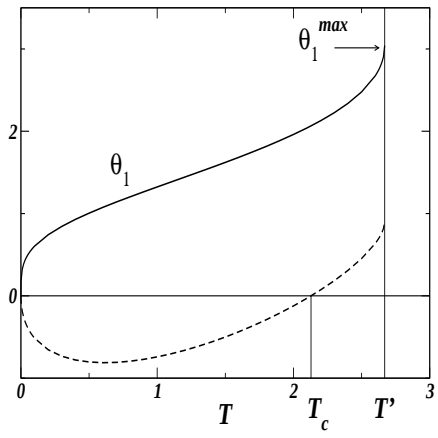

Figure 4.7: The solid line: θ_1 as a function of parameter T [defined in eqn. (4.6.37)] for $g = 0$. The dashed line: the plot of function $T - 2\theta_1^2(T)/\cosh\theta_1(T)$ versus T. The maximum value of θ_1 at $T = T'$ is indicated.

soliton width, σ. A plot of θ_1 as a function of T is presented in Fig. (4.7), where the maximum value of θ_1 is $\theta_1^{\max} \approx 3.0415$. The minimum at θ_1 is a global one if $E(\theta_1) < \epsilon/2$; using eqn. (4.2.23), this condition reads

$$T - \frac{2\theta_1^2(T)}{\cosh\theta_1(T)} \; < \; 0. \tag{4.6.38}$$

As one can see from Fig. (4.7), condition (4.6.38) is satisfied for $T < T_c$, where $T_c \simeq 2.1289$: then, a global minimum exists only for $0 < T < T_c$, while for $T_c < T < T'$ the minimum is local, corresponding to a metastable state. Using the value of T_c and definition (4.6.36), one arrives at eqn. (4.3.26).

For $g > 0$ (recall it corresponds to the two-body repulsion), variational energy (4.2.23) for $c > c^*$ does not have a minimum at finite values of σ. However, for $c = c^*$ a finite minimum is possible. Indeed, with definition of

G as per eqn. (4.4.27), condition $\partial E/\partial\sigma = 0$ can be written as

$$G \;=\; \theta^2 \frac{\sinh\theta}{\cosh^2\theta}. \tag{4.6.39}$$

For $G < G' \approx 1.0341$, eqn. (4.6.39) has two roots. By imposing the condition that the value of the energy at $\sigma = \sigma_1$ is smaller than $\epsilon/2$, one gets $G < G_c \simeq 0.6627$. Then, similar to the situation considered above, a global minimum exists only $0 < G < G_c$, while for $G_c < G < G'$ the minimum is local.

For $c < c^*$, condition $\partial E/\partial\sigma = 0$ reads

$$T \;=\; \theta^3 \frac{\sinh\theta}{\cosh^2\theta} - G\theta. \tag{4.6.40}$$

One can see that condition (4.6.40) is satisfied for $T < T'(G)$, with $T'(G') = 0$. Then, for $G > G'$, i.e., for ϵ small enough, the variational energy does not have a minimum. Imposing the condition that the minimum is global leads to $T < T_c$, with $T_c(G_c) = 0$. Then, for $G > G_c$, i.e. for ϵ smaller than a critical value, the variational energy cannot have a *global* minimum for a finite value of σ, i.e., localized states. Functions $T'(G)$ and $T_c(G)$ are plotted in Fig. (4.8); in Fig. (4.9), we plot maximum value $\theta_1^{\max}$ of θ_1 for $T = T'(G)$, as a function of G.

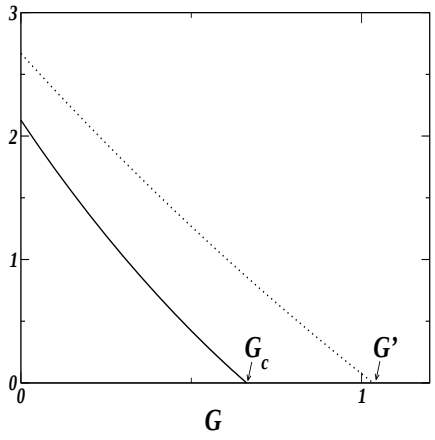

Figure 4.8: The solid (dashed) line: the plot of T_c (T') as a function of parameter G.

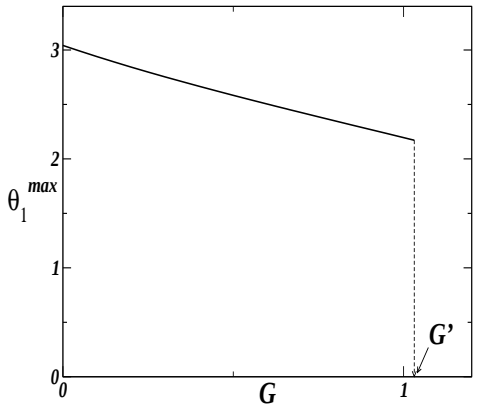

Figure 4.9: The plot of maximum value $\theta_1^{\max}$ of the smaller root of eqn. (4.6.37), θ_1 [at $T = T'(G)$], as a function of G.

Conclusions and Outlook

In this thesis we have analyzed one-dimensional Bose gases with N-body local attractive interactions.

By using a mean-field approach, we found that, in the homogeneous case, $N = 3$ is a critical point, and that bright soliton solutions are possible only for a specific value of the interaction strength c^*. At this critical value, an infinite degeneracy occurs: this degeneracy is parametrized by the chemical potential μ, i.e. eigenfunctions with the same negative μ have the same energy. For $N < 3$, the bright soliton coincides with the ground state of the Gross-Pitaevskii equation: in particular, as $N \to 3^-$ the soliton width tends to diverge when $c < c^*$ or to vanish when $c > c^*$.

We have also discussed how a harmonic trap can stabilize this bound state. The result of our variational analysis was that a localized state is possible only if the interaction strength is smaller than the homogeneous critical value c^*, while for $c \geq c^*$ the collapse cannot be prevented even for very large trap frequency. We discussed also the role played by the dimension for N-body local attractive interactions, showing that higher body interactions lead to more unstable solitons in higher dimensions. We remark that the analysis of two-body nonlocal attractive interactions has revealed different ranges of stability with respect to the local ones [47]: we expect that, for 3- and N-body interactions, this effect may become even more relevant, and thus object of future investigations.

The second issue we have addressed within this study is the effect of an

optical lattice (OL) on the ground state properties of 1D Bose gases with attractive three-body and repulsive two-body interactions, described by the GPE (Gross-Pitaevskii equation) with the CQ (cubic-quintic) nonlinearity.

We have demonstrated that the OL opens a stability window for the solitons, provided that the OL strength ϵ exceeds a finite minimum value. The size of the window depends on ϵ/q^2, where q is the OL's wavenumber. We have also considered the effects of the additional harmonic trap, finding that, if the quintic nonlinearity is strong enough ($c \geq c^*$), a metastability region may arise, depending on the matching between minima of the periodic potential and harmonic trap.

A very interesting perspective comes from the recent proposals to realize experimentally ultracold boson systems which are described by effective Hamiltonians with three-body interaction terms [19, 21]. Indeed, an experimental realization of these systems would open the possibility to test the stationary properties we have found for the three-body systems and assess, at the same time, the validity of the Gross-Pitaevskii approximation. In this respect, the possibility to induce and tune effective 3-body interactions may become an important tool to control the nonlinear dynamical properties of localized wave-packets propagating in optical lattices: in this context, we believe that our results may provide a useful theoretical framework.

Acknowledgments

Bibliography

[1] M. H. Anderson, J. R. Ensher, M.R. Matthews, C. E. Wieman and E. A. Cornell, Science **269**, 198 (1995).

[2] L. P. Pitaevskii and S. Stringari, *Bose-Einstein Condensation* (Oxford, Clarendon Press, 2003).

[3] C. J. Pethick and H. Smith, *Bose-Einstein Condensation in Dilute Alkali Gases* (Cambridge, Cambridge University Press, 2002).

[4] B. DeMarco and D. S. Jin, Science **285**, 1703 (1999).

[5] A. K. Truscott, K. E. Strecker, W. McAlexander, G. B. Partridge and R. G. Hulet, Science **291**, 2570 (2001).

[6] A. J. Leggett, Rev. Mod. Phys. **72**, 307 (2001)

[7] http://www.nanopicoftheday.org/2004Pics/March2004/BEC.htm

[8] H. Feshbach, Ann. Phys. **19**, 287 (1962).

[9] T. Giamarchi, arXiv:cond-mat/0605472

[10] E.H. Lieb and W. Liniger, Phys. Rev. **130**, 1605 (1963); E.H. Lieb, Phys. Rev. **130**, 1616 (1963).

[11] D.C. Mattis, *The many-body problem: an encyclopedia of exactly solved models in one dimension*, Singapore, World Scientific, 1993.

[12] M. Girardeau, Jour. Math. Phys., **1**, 516 (1960).

[13] T. Giamarchi, *Quantum physics in one dimension*, Oxford University Press 2004.

[14] M. Kohl, H. Moritz, T. Stoferle, C. Schori, and T. Esslinger, J. Low Temp. Phys. **138**, 635 (2005).

[15] M. Olshanii, Phys. Rev. Lett. **81**, 938 (1998).

[16] B. Paredes, A. Widera, V. Murg, O. Mandel, S. Folling, I. Cirac, G.V. Shlyapnikov, T.W. Hansch, and I Bloch, Nature **429**, 277 (2004).

[17] T. Kinoshita, T. Wenger, and D.S. Weiss, Science **305**, 1125 (2004).

[18] A.H. van Amerongen, J.J.P. van Es, P. Wicke, K.V. Kheruntsyan, N.J. van Druten, arXiv:0709.1899.

[19] H. P. Buchler, A. Micheli, and P. Zoller, Nature Phys.**3**, (2007) 726

[20] N.R. Cooper, Phys. Rev. Lett. **92**, 220405 (2004).

[21] B. Paredes, T. Keilmann, and J. I. Cirac, Phys. Rev. A **75**, (2007) 053611.

[22] G. Moore and N. Read, Nucl. Phys. B **360**, (1991) 362.

[23] A.Y. Kitaev, Ann. Phys. (N.Y.) **303**, 2 (2003).

[24] V.E Zakharov and V.S. Synakh, Sov. Phys. JETP **41**, 465 (1975).

[25] M. J. Ablowitz, B. Prinari, and A. D. Trubatch, *Discrete and Continuous Nonlinear Schrödinger Systems* (Cambridge, University Press, 2004).

[26] L.D. Carr, C.W. Clark, W.P. Reinhardt, Phys. Rev. A **62**, 063610 (2000).

[27] L.D. Carr, C.W. Clark, W.P. Reinhardt, Phys. Rev. A **62**, 063611 (2000).

[28] C. Sulem and P.-L. Sulem, *The Nonlinear Schrödinger Equation* (Springer-Verlag, New York, 1999)

[29] B. A. Malomed, *Soliton Management in Periodic Systems* (Springer-Verlag, New York, 2006).

[30] L. Salasnich, A. Parola and L. Reatto, Phys. Rev. A **65**, (2002) 043614.

[31] E. Fersino, G. Mussardo, and A. Trombettoni, Phys. Rev.A **77**, (2008) 053608.

[32] A. L. Fetter, arXiv:cond-mat/9510037.

[33] P. A. Ruprecht, M. J. Holland, K. Burnett, and M. Edwards, Phys. Rev. A **51**, (1995) 4704

[34] Q. Chen, J. Stajic, S. T. and K. Levin, arXiv:cond-mat/0404274v3.

[35] K. E. Strecker, G. B. Partridge, A. G. Truscott, and R. G. Hulet, Nature **417**, (2002) 150.

[36] S. L. Cornish, N. R. Claussen, J. L. Roberts et al., Phys. Rev. Lett. **85**, (2000) 1795.

[37] L. Khaykovich, F. Schreck, G. Ferrari, T. Bourdel, J. Cubizolles, L. D. Carr, Y. Castin, and C. Salomon, Science **296**, (2002) 1290.

[38] N. K. Wilkin, J. M. F. Gunn, R. A. Smith, Phys. Rev. Lett. **80**, (1998) 2265.

[39] J. M. Gerton, D. Strekalov, I. Prodan et al., Nature **408** (2000) 692.

[40] Y. Kagan, A. E. Muryshev, G. V. Shlyapnikov, Phys. Rev. Lett. **81** (1998) 933.

[41] H. Saito and M. Ueda, Phys. Rev. Lett. **90** (2003) 040403.

[42] R. J. Dodd, M. Edwards, C. J. Williams et al., Phys. Rev. A **54** (1996) 661.

[43] L. S. Cederbaum, A. I. Streltsov and O. E. Alon, Phys. Rev. Lett. **100** (2008) 040402

[44] L. Salasnich, A. Parola and L. Reatto, Phys. Rev. A **59** (1999) 2990.

[45] L. Salasnich, A. Parola and L. Reatto, Phys. Rev. A **66** (2002) 043603.

[46] L. Salasnich, A. Parola and L. Reatto, Phys. Lett. **91** (2003) 080405.

[47] A. Parola, L. Salasnich, and L. Reatto, Phys. Rev. A **57**, R3180 (1998).

[48] T. Stöferle, H. Moritz, C. Schori, M. Köhl andT. Esslinger, Phys. Rev. Lett., **92**, 130403 (2004).

[49] T. Kinoshita, T. Wenger and D. S. Weiss, Science, **305**, 1125 (2004).

[50] Paredes *et al.*, Nature, **429**, 277 (2004).

[51] W. Zwerger, J. Opt. B: Quantum Semiclass. Opt., **5**, 9 (2003)

[52] F. Franchini's lecture notes *Notes on Bethe Ansatz techniques*, delivered at SISSA, March-April 2008

[53] C. N. Yang and C. P. Yang, J. Math. Phys. **10**, 1115 (1969). Proc. Roy. Soc. Lond. A 260 (1961) 127; Proc. Roy. Soc. Lond. A 262 (1961) 237.

[54] V.E. Korepin, N.M. Bogoliubov, and A.G. Izergin, *Quantum inverse scattering method and correlation functions*, Cambridge, University Press, 1993.

[55] S.L. Cornish, S.T. Thompson, and C.E. Wieman, Phys. Rev. Lett. **96**, 170401 (2006).

[56] P.G. Kevrekidis, D.J. Frantzeskakis, and R. Carretero-Gonzalez eds., *Emergent Nonlinear Phenomena in Bose-Einstein Condensates*, Springer Series on Atomic, Optical, and Plasma Physics, 2007.

[57] G. Baym and C. J. Pethick, Phys. Rev. Lett. **76**, (1996) 6

[58] F. Calogero and A. Degasperis, Phys. Rev. A **11**, (1975) 265

[59] F.D.M. Haldane, J. Phys. C: Solid State Phys. **14**, 2585 (1981).

[60] A.O. Gogolin, A.A. Nersesyan, and A.M. Tsvelik, *Bosonization and strongly correlated systems*, Cambridge, University Press, 1998.

[61] M.A. Cazalilla, J. Phys. B **37**, S1 (2004).

[62] J. B. McGuire, J. Math. Phys. **5**, (1964) 622

[63] P. Calabrese and J.-S. Caux, Phys. Rev.A **74**, 031605 (2006);

[64] P. Calabrese, J.-S. Caux and N.A. Slavnov , J. Stat. Mech. **0701**, 008 (2007);

[65] P. Calabrese and J.-S. Caux, Phys. Rev. Lett. **98**, 150403 (2007); J. Stat. Mech. P08032 (2007).

[66] A. Kundu, Phys. Rev. Lett. **83**, 1275 (1999).

[67] E.A. Kuznetsov, A.M. Rubenchik, and V.E. Zakharov, Phys. Rep. **142**, 103 (1986).

[68] Yu. S. Kivshar and B. A. Malomed, Rev. Mod. Phys.**61**, 763 (1989).

[69] D. Mihalache, M. Bertolotti, and C. Sibilia, Prog. Opt. **27**, 229 (1989).

[70] A.W. Snyder and D.J. Mitchell, Opt. Lett. **18**, 101 (1993).

[71] J.M. Christian, G.S. McDonald, R.J. Potton, and P. Chamorro-Posada, Phys. Rev. A **76**, 033834 (2007).

[72] A. Smerzi and A. Trombettoni, Phys. Rev. A **68**, 023613 (2003).

[73] M. J. Ablowitz and H. Segur, *Solitons and the Inverse Scattering Transform* (SIAM, Philadelphia, 1981)

[74] A. D. Polyanin and V. F. Zaitsev, *Handbook of Nonlinear Partial Differential Equations* (Boca Raton, Chapman & Hall/CRC Press, 2004)

[75] F. Merle and P. Raphael, Invent. Math. **156**, 565 (2004).

[76] M. G. Vakhitov and A. A. Kolokolov, Radiophys. Quantum Electron. **16**, (1973) 783

[77] M.I. Weinstein, Comments Pure Appl. Math. **39**, 51 (1986).

[78] D.E. Pelinovsky, V.V. Afanasjev, and Yu. S. Kivshar, Phys. Rev. **53**, 1940 (1996).

[79] O. Morsch and M. K. Oberthaler, Rev. Mod. Phys. **78**, (2006) 179

[80] A. Trombettoni and A. Smerzi, Phys. Rev. Lett.**86**, (2001) 2353

[81] F. Kh. Abdullaev, B. B. Baizakov, S. A. Darmanyan, V. V. Konotop, and M. Salerno, Phys. Rev. A **64**, (2001) 043606

[82] G. L. Alfimov, P. G. Kevrekidis, V. V. Konotop, and M.Salerno, Phys. Rev. E **66**, (2002) 046608

[83] M. A. Porter, R. Carretero-González, P. G. Kevrekidis and B. A. Malomed, Chaos **15** (2005) 015115.

[84] B. Wu and Q. Niu, Phys. Rev. A **64**, (2001) 061603(R)

[85] A. Smerzi, A. Trombettoni, P. G. Kevrekidis, and A. R. Bishop, Phys. Rev. Lett. **89**, (2002) 170402

[86] V. V. Konotop and M. Salerno, Phys. Rev. A **65**,(2002) 021602

[87] B. Wu and Q. Niu, New J. Phys. **5**, (2003) 104

[88] C. Menotti, A. Smerzi, and A. Trombettoni, New J. Phys.**5**, (2003) 112

[89] E. Taylor and E. Zaremba, Phys. Rev. A **68**,(2003) 053611

[90] M. Krämer, C. Menotti, L. P. Pitaevskii, and S. Stringari, Eur. Phys. J. D **27**, (2003) 247

[91] M. Krämer, C. Menotti and M. Modugno, J. Low Temp. Phys. **138**, (2005) 729

[92] F. S. Cataliotti, L. Fallani, F. Ferlaino, C. Fort, P. Maddaloni, and M. Inguscio, New J. Phys. **5**, (2003) 71

[93] L. Fallani, L. De Sarlo, J. E. Lye, M. Modugno, R. Saers, C.Fort, and M. Inguscio, Phys. Rev. Lett. **93**, (2004) 140406

[94] B. Eiermann, T. Anker, M. Albiez, M. Taglieber, P. Treutlein, K. P. Marzlin, and M. K. Oberthaler, Phys. Rev. Lett. **92**, (2004) 230401

[95] B. B. Baizakov, B. A. Malomed, and M. Salerno, Europhys. Lett., **63**, (2003) 642

[96] J. Yang and Z. H. Musslimani, Opt. Lett. **28** (2003) 2094

[97] F. Kh. Abdullaev and M. Salerno, Phys. Rev. A **72**, (2005) 033617

[98] L. Khaykovich and B. A. Malomed, Phys. Rev. A **74**, (2006) 023607

[99] A. E. Muryshev, G. V. Shlyapnikov, W. Ertmer, K. Sengstock, and M. Lewenstein, Phys. Rev. Lett. **89** (2002) 110401

[100] Yu. S. Kivshar and G. P. Agrawal, *Optical Solitons* (Elsevier Science, San Diego, 2003)

[101] B. A. Malomed, Z. H. Wang, P. L. Chu, and G. D. Peng, J. Opt. Soc. Am. B, **16**, (1999) 1197

[102] Z. Xu, Y. V. Kartashov, and L. Torner, Phys. Rev. Lett. **95**, (2005) 113901

[103] Z. Dai, Y. Wang, and Q. Guo, Phys. Rev. A **77**, (2008) 063834

[104] B. B. Baizakov, B. A. Malomed and M. Salerno, Phys. Rev. A **70** (2004) 053613; Phys. Rev. E **74** (2006) 066615 (2006).

[105] D. Mihalache, D. Mazilu, F. Lederer, Y. V. Kartashov, L.-C. Crasovan, and L. Torner, Phys. Rev. E **70** (2004) 055603(R)

[106] Yu. B. Gaididei, J. Schjodt-Eriksen, and P. L. Christiansen, Phys. Rev. E **60**, (1999) 4877

[107] Kh. I. Pushkarov, D. I. Pushkarov, and I. V. Tomov, Opt. Quantum Electron. **11**, (1979) 471

[108] S. Cowan, R. H. Enns, S. S. Rangnekar, and S. S. Sanghera, Can. J. Phys. **64**, (1986) 311

[109] B. A. Malomed, Progr. Opt. **43**, (2001) 69

[110] D. Anderson, Phys. Rev. A **27**, (1983) 3135

[111] B. B. Baizakov and M. Salerno, Phys. Rev. A **69**, (2004) 013602